A Study of the Portable and Fully Automated Artificial Kidney

Jianya Wei

A thesis submitted in partial fulfillment of the requirements for the degree of

Master of Science in Mechanical Engineering

University of Washington

2026

Committee:

Dayong Gao

Jae Hyun Chung

Ruidong Ma

Program Authorized to Offer Degree:

Mechanical Engineering

University of Washington

Abstract

A Study of the Portable and Fully Automated Artificial Kidney

Jianya Wei

Chair of the Supervisory Committee:
Professor Dayong Gao
Mechanical Engineering

Extracorporeal blood purification systems are essential for the treatment of renal and hepatic dysfunction, but their effectiveness depends on both biochemical toxin removal and reliable engineering performance. Conventional dialysis is effective for small water-soluble solutes, but it is limited in the removal of strongly protein-bound toxins because only the unbound toxin fraction can readily cross the dialysis membrane. In addition, compact and portable dialysis systems require stable fluid delivery, accurate flow regulation, simplified circuit setup, and integrated safety mechanisms. This thesis investigates these challenges through the development and evaluation of a portable and fully automated artificial kidney platform.

The first part of this work evaluates albumin dialysis as a strategy for removing representative protein-bound toxins. An in vitro albumin dialysis circuit was used to compare polysulfone and cellulose dialyzers over a 3-hour treatment period. Indoxyl sulfate and bilirubin were selected as representative toxins, and bovine serum albumin was monitored to assess albumin retention and solution stability. Both membrane groups showed rapid initial indoxyl sulfate reduction, especially within the first 0.5 hour, followed by a slower approach toward a quasi-steady state. Bilirubin removal also occurred over the course of treatment, with the polysulfone membrane generally showing stronger bilirubin transfer at later time points. In all membrane trials, bovine serum albumin concentrations remained within a relatively narrow range, indicating stable albumin retention during the experiment.

The second part of this work focuses on flow regulation in the artificial kidney system. Pump calibration experiments established a linear relationship between rotational speed and flow rate for the selected tubing and pump configurations. A closed-loop proportional-integral control strategy was then implemented to improve the stability and volumetric accuracy of the replacement and ultrafiltration channels. Open-loop operation produced persistent flow offsets and large cumulative-error drift, while pure integral control reduced drift but introduced oscillatory behavior. Optimized channel-specific PI gains provided the best overall performance, maintaining both channels close to the 40 mL/min target and limiting cumulative error without sustained drift or large oscillation.

The final part of this thesis presents the design and integration of a portable dialysis prototype. The system combines a compact acrylic and 3D-printed structure, cassette-based fluidic organization, integrated scales, pump controllers, RS-485 communication, and a bubble-detection-based safety shutdown mechanism. Together, the albumin dialysis experiments, flow-control evaluation, and prototype design demonstrate the feasibility of a compact automated platform for membrane-based extracorporeal support. This work provides an engineering foundation for future development of portable artificial kidney systems with improved toxin-removal capability, fluid-control accuracy, and operational reliability.

TABLE OF CONTENTS

LIST OF FIGURES

LIST OF TABLES

GLOSSARY

ALBUMIN DIALYSIS: A dialysis strategy in which albumin is added to the dialysate side to provide binding capacity for protein-bound toxins that cross the dialysis membrane.

ALBUMIN DIALYSATE: Dialysate supplemented with albumin so that protein-bound toxins crossing the membrane can bind on the dialysate side and maintain a favorable transfer gradient.

ARTIFICIAL KIDNEY: An extracorporeal blood purification system designed to remove toxins and regulate fluid balance when kidney function is impaired or when artificial renal replacement support is needed.

BILIRUBIN: A hydrophobic, strongly albumin-bound hepatic toxin used in this thesis as a representative larger protein-bound solute for albumin dialysis evaluation.

BLOOD-SIDE SOLUTION: The experimental solution circulated through the blood compartment of the dialyzer. In the albumin dialysis experiments, this solution contained BSA and the representative toxins.

BSA: Bovine serum albumin, a model albumin protein used in this thesis to prepare albumin-containing solutions and to evaluate albumin retention during dialysis experiments.

CELLULOSE DIALYZER: A dialyzer using a cellulose-based membrane material. In this thesis, cellulose dialyzers were compared with polysulfone dialyzers for albumin dialysis performance.

CLOSED-LOOP CONTROL: A control approach in which feedback measurements are used to adjust system operation in real time. In this thesis, scale-based flow measurements were used to adjust pump speed.

CUMULATIVE ERROR: The accumulated difference between the target delivered volume and the measured delivered volume over time. It is used as an indicator of long-term volumetric accuracy.

DIALYSATE-SIDE RESERVOIR: The container holding the dialysate solution during the in vitro albumin dialysis experiment. Samples from this reservoir were used to evaluate toxin accumulation and BSA stability.

DIALYSATE: The fluid used on the opposite side of the dialysis membrane from the blood-side solution. It receives solutes that diffuse or transfer across the membrane.

DIALYZER: A membrane-based device that separates two fluid streams and enables solute transport across a semipermeable membrane.

EXTRACORPOREAL CIRCUIT: A fluidic circuit that circulates blood or a blood-side substitute outside the body through pumps, tubing, sensors, and purification components.

FLOW RATE: The volume of fluid delivered per unit time. In this thesis, flow rate is typically reported in mL/min.

HEPATIC TOXIN: A toxin associated with impaired liver function or liver failure. Bilirubin is used in this thesis as a representative hepatic toxin.

INDOXYL SULFATE: A representative protein-bound uremic toxin used in this thesis to evaluate albumin dialysis performance.

INTEGRAL CONTROL: The component of a PI controller that responds to accumulated past error and helps reduce steady-state deviation.

LSTM: Long short-term memory, a recurrent neural-network architecture used to learn temporal patterns from sequential flow-control data.

MASS TRANSFER: The movement of solute between the blood-side and dialysate-side compartments. In dialysis, mass transfer is influenced by concentration gradients, membrane properties, flow conditions, and protein binding.

MEMBRANE MATERIAL: The material forming the semipermeable barrier inside a dialyzer. This thesis compares cellulose and polysulfone membranes for toxin removal and albumin retention.

OPEN-LOOP CONTROL: A control approach in which the pump operates at a prescribed command without real-time feedback correction.

PERISTALTIC PUMP: A pump that moves fluid by compressing flexible tubing with rotating rollers. It is commonly used in extracorporeal circuits because the fluid remains contained inside the tubing.

PI CONTROL: Proportional-integral control, a feedback control method that combines proportional response to current error with integral response to accumulated error.

POLYSULFONE DIALYZER: A dialyzer using a polysulfone membrane material. In this thesis, polysulfone dialyzers were evaluated for protein-bound toxin removal and albumin retention.

PRIMING: The process of filling the fluidic circuit with solution before operation to remove air and prepare the system for stable circulation.

PROTEIN-BOUND TOXIN: A toxin that is strongly associated with plasma proteins such as albumin. These toxins are difficult to remove by conventional dialysis because only the unbound fraction can readily cross the membrane.

PROPORTIONAL CONTROL: The component of a PI controller that responds directly to the current difference between the target flow rate and the measured flow rate.

QUASI-STEADY STATE: A condition in which measured concentrations change slowly over time after an initial transient response. In the albumin dialysis experiments, IS approached a quasi-steady level after the rapid early decrease.

REPLACEMENT PUMP: The pump responsible for delivering replacement fluid in the flow-control experiments. It is abbreviated as RP in this thesis.

RP: Replacement pump or replacement channel.

RS-485: A serial communication standard used in the prototype to communicate with pump controllers over a robust multi-device bus.

SEMIPERMEABLE MEMBRANE: A membrane that allows selected solutes and water to pass while restricting larger components such as albumin, depending on membrane properties and operating conditions.

STANDARD DEVIATION: A measure of variability among replicate experiments. Error-bar plots in this thesis report mean concentration values with standard deviation.

TOXIN TRANSFER: Movement of toxin from the blood-side solution into the dialysate compartment during dialysis.

TV-MTLSTM: Total-variation-regularized multi-head long short-term memory, the learning framework used in this thesis to predict channel-specific PI gains from flow-control time-series data.

ULTRAFILTRATION: The removal of fluid across a membrane, usually driven by pressure difference. In this thesis, ultrafiltration is associated with the waste or fluid-removal channel.

UF: Ultrafiltration pump or ultrafiltration channel.

ACKNOWLEDGMENTS

I would like to express my sincere gratitude to my advisor, Professor Dayong Gao, for his guidance, support, and encouragement throughout my master's study. I am especially grateful to him for giving me the opportunity to join his laboratory and participate in meaningful research in biomedical engineering and artificial organ systems. His advice, expertise, and high standards have been invaluable to the development and completion of this thesis.

I would also like to thank my thesis committee members for their time, feedback, and helpful suggestions. Their comments and guidance helped me improve both the quality of this thesis and my understanding of the research.

I am deeply grateful to the members of the Center for Cryo-Biomedical Engineering and Artificial Organs for their assistance, discussions, and support during my research. Working in this group has been a valuable learning experience, and I truly appreciate the collaborative and supportive environment in the laboratory. In particular, I would like to thank Shaohang, Tianpu, and Nanye for their help, encouragement, and many useful discussions throughout my project.

Finally, I would like to thank my family and friends for their constant encouragement, understanding, and support throughout my graduate study. Their support has been an important source of strength during this journey.

Chapter 1

INTRODUCTION

1.1 Background and Motivation

Extracorporeal blood purification has become an essential therapeutic strategy for patients with severe renal or hepatic dysfunction. Conventional dialysis is highly effective for the removal of water-soluble toxins, excess electrolytes, and fluid through concentration-driven transport across a semipermeable membrane. However, many clinically important toxins are strongly bound to carrier proteins in blood, especially albumin, and therefore cannot be removed efficiently by traditional dialysis [1]. Because the carrier protein cannot cross the membrane, only the small free fraction of a protein-bound toxin is immediately available for diffusive transport, which severely limits overall clearance [2]. This limitation is particularly important in liver failure, cholestasis, and chronic kidney disease, where toxins such as bilirubin, bile acids, and protein-bound uremic solutes can accumulate and contribute to disease progression [3].

To overcome this limitation, albumin-based dialysis has been developed as a strategy to enhance the removal of protein-bound toxins. In this approach, albumin or another binding agent is introduced on the dialysate side to capture toxin molecules that cross the membrane, thereby maintaining a favorable concentration gradient and promoting continued dissociation of toxin from albumin in the blood [4]. Existing extracorporeal liver support systems, including single-pass albumin dialysis, recirculating albumin dialysis, and sorbent-regenerated albumin circuits, have demonstrated the feasibility of this concept [5]. Nevertheless, these systems remain limited by high albumin consumption, circuit complexity, regeneration requirements, and variable clinical performance. Previous studies from our laboratory have further shown that toxin removal in albumin dialysis depends not only on membrane prop-

erties and toxin–albumin binding, but also on operating conditions such as dialysate composition and flow rate, underscoring the importance of engineering optimization in addition to biochemical feasibility [6].

In parallel with toxin-removal performance, reliable fluid handling is a fundamental requirement for any dialysis-based support system. Even when the biochemical mechanism for toxin transfer is effective, unstable or inaccurate flow delivery can degrade treatment consistency, alter mass transfer conditions, and introduce accumulated volumetric error over long operating periods [7]. This issue is particularly relevant for compact or prototype dialysis platforms, in which pump characteristics, tubing compliance, and transient disturbances may cause deviations between nominal and actual flow rates [8]. As a result, precise calibration and closed-loop control of fluid transport are essential not only for treatment accuracy, but also for overall system robustness and future clinical translation [9].

Motivated by these challenges, this thesis investigates two complementary aspects of extracorporeal support system development. The first is the feasibility of albumin-based dialysis for the removal of representative protein-bound toxins, with particular emphasis on the transport behavior of indoxyl sulfate and bilirubin and on the retention or stability of albumin within the system. The second is the engineering problem of flow regulation in a dialysis platform, where stable and accurate pump control is required to maintain intended operating conditions over extended periods. Although these two studies address different experimental questions, they are united by a common objective: to improve the functionality and practicality of membrane-based extracorporeal support technologies for toxin removal and fluid management.

1.2 Protein-Bound Toxins and Albumin Dialysis

1.2.1 Clinical Significance and Removal Challenges of Protein-Bound Toxins

Liver failure remains a major cause of morbidity and mortality worldwide and continues to place a substantial burden on clinical care. In both acute and chronic settings, progressive

loss of hepatic function disrupts the liver's essential metabolic, synthetic, and excretory roles, often leading to jaundice, coagulopathy, hepatic encephalopathy, and multi-organ dysfunction [10]. Although liver transplantation remains the standard treatment for end-stage liver failure, its use is limited by donor organ shortage, delayed access, and the fact that many critically ill patients deteriorate before transplantation can be performed. These challenges have driven continued interest in extracorporeal liver support as a bridge to transplantation or, in some cases, a bridge to recovery [3, 5].

A key feature of liver failure is the accumulation of toxins that would normally be cleared or metabolized by a healthy liver [11]. Among them, a clinically significant group includes hydrophobic and strongly protein-bound compounds such as bilirubin, bile acids, and other albumin-associated toxins. Because these solutes are extensively bound to albumin in the circulation, only a limited free fraction is available for transport, which greatly restricts their removal by conventional dialysis [12]. Their retention contributes not only to abnormal laboratory findings but also to broader systemic injury, including oxidative stress, inflammation, endothelial dysfunction, and further damage to extrahepatic organs [13]. For this reason, protein-bound toxins are closely linked to both the severity and progression of liver failure.

The removal of protein-bound toxins remains a major challenge in extracorporeal blood purification [1]. Unlike small water-soluble solutes, these toxins are not freely dissolved in plasma but are extensively associated with carrier proteins, most notably albumin. As a result, only the unbound fraction is immediately available for transport across the dialysis membrane, and even after this fraction is removed, the bound fraction must first dissociate from its carrier protein before further clearance can occur [14]. This binding equilibrium largely explains why conventional dialysis is often ineffective for strongly protein-bound compounds [15]. The difficulty is further compounded by the physicochemical properties of clinically relevant toxins: some, such as indoxyl sulfate, are small in molecular size but exhibit strong albumin binding, whereas others, such as bilirubin, combine strong protein association with hydrophobicity and more complex transport behavior [14, 4]. In both cases, toxin removal depends not only on membrane permeability, but also on protein-toxin dissociation

kinetics, the concentration gradient across the membrane, and the capacity of the dialysate side to continuously accept and retain the transferred toxin.

In addition to these biochemical constraints, practical engineering factors also influence toxin removal. Dialysate composition, membrane material, flow configuration, and operating flow rates can all affect the extent of toxin transfer [6]. If the dialysate side does not provide a sufficient binding sink, the transmembrane driving force rapidly decreases and toxin removal becomes limited [16]. Similarly, mechanical variables such as unstable pump delivery, flow disturbances within the fluidic circuit, or poorly controlled operating conditions may alter mass transfer performance and reduce treatment consistency over time [17]. These considerations show that the removal of protein-bound toxins is not solely a membrane problem, but rather a coupled transport and system-design challenge. For these reasons, effective clearance requires approaches that go beyond conventional dialysis [1, 18]. Strategies such as albumin-containing dialysate, adsorptive detoxification, and other enhanced extracorporeal support methods have been developed to address these limitations. Understanding the transport barriers associated with representative toxins is therefore essential for the design of more effective blood purification systems.

1.2.2 Existing Detoxification Strategies and Their Engineering Limitations

Because conventional dialysis is fundamentally driven by diffusive and convective transport, a variety of enhanced detoxification strategies have been developed to improve the removal of strongly protein-bound toxins [1]. Although these approaches differ in mechanism, they all attempt to overcome the limited clearance imposed by strong toxin–albumin binding and restricted transmembrane transport [16].

Conventional renal replacement therapies, including hemodialysis and hemofiltration, are highly effective for the removal of water-soluble solutes and for fluid management. However, as discussed previously, their performance is inherently limited for strongly albumin-bound species because only the unbound toxin fraction is immediately available for transport across the membrane [15]. Without a dedicated binding sink on the dialysate side, the trans-

membrane concentration gradient declines rapidly, making these methods insufficient for the effective removal of many hepatic toxins and protein-bound uremic solutes [19].

To address this limitation, adsorption-based approaches such as hemoperfusion have been introduced to capture toxins directly from blood or plasma [20]. These methods can improve removal for selected compounds, but their performance depends strongly on sorbent properties, adsorption capacity, and compatibility with the extracorporeal circuit. In addition, sorbent saturation and the need for replacement or regeneration complicate prolonged operation and reduce the simplicity of the treatment platform [21].

Exchange-based methods, such as plasma exchange, provide a more direct means of removing albumin-bound toxins by replacing the toxin-carrying plasma fraction itself [16]. Although this approach can achieve broad toxin removal, it is resource-intensive and requires substantial volumes of donor plasma or replacement fluids. Its dependence on external blood products and careful volume management also limits its practicality as a continuous support strategy [22].

Among these modalities, albumin dialysis has emerged as one of the most important approaches for extracorporeal removal of protein-bound toxins [23]. By using albumin-enriched dialysate, albumin dialysis provides a binding sink across the membrane, thereby promoting continued transfer of albumin-associated toxins from the blood side and helping sustain the driving force for clearance [4, 18]. This principle is particularly relevant to the removal of bilirubin, bile acids, and other strongly protein-bound solutes.

Despite its biochemical promise, albumin dialysis remains subject to important engineering limitations. System performance depends not only on toxin binding and dialysate composition, but also on membrane characteristics, dialyzer configuration, and operating flow conditions [6]. Different dialyzers may exhibit different transport behavior, toxin removal efficiency, and protein retention performance, even under similar operating conditions [24, 25]. As a result, the design of an effective detoxification system cannot rely solely on the choice of detoxification strategy; it must also account for how the membrane and dialyzer influence mass transfer within the extracorporeal circuit. These considerations motivate the

evaluation of dialyzer performance as an essential step in the development of more effective albumin-based blood purification systems.

1.2.3 Principles and Limitations of Albumin Dialysis

Albumin dialysis was developed to improve the extracorporeal removal of strongly protein-bound toxins that cannot be cleared efficiently by conventional dialysis. The core principle is to introduce albumin, or an equivalent binding environment, on the dialysate side so that toxins crossing the membrane can be selectively captured [4]. By continuously removing the transferred toxin from the free phase of the dialysate, this approach helps preserve the transmembrane concentration gradient and promotes further dissociation of toxin from albumin in the blood [26]. As a result, albumin dialysis extends the applicability of membrane-based purification to compounds such as bilirubin, bile acids, and other albumin-associated solutes [27].

In practical systems, this principle has been implemented in several forms, including single-pass albumin dialysis, recirculating albumin dialysis, and albumin circuits combined with sorbent regeneration [18, 5, 28]. Although these configurations differ in circuit design, they share the same transport objective: to sustain toxin removal by maintaining a sufficient binding sink on the dialysate side. Consequently, albumin dialysis performance depends not only on toxin–albumin binding and membrane permeability, but also on dialysate composition, dialyzer characteristics, and operating flow conditions [18].

Despite its biochemical promise, albumin dialysis remains associated with important limitations. In single-pass systems, albumin consumption can be substantial, which increases treatment cost and reduces practicality for prolonged use. In recirculating systems, the need for sorbent regeneration and additional circuit components increases system complexity and may introduce greater variability in operation [18, 29]. Moreover, treatment performance is influenced by membrane selection and dialyzer configuration, meaning that toxin removal and protein retention may vary even under similar nominal operating conditions [24]. These limitations indicate that successful albumin dialysis depends not only on the detoxification

concept itself, but also on how effectively the extracorporeal system is engineered to support stable and efficient mass transfer [25].

For these reasons, albumin dialysis should be viewed as both a biochemical and an engineering problem. Its effectiveness relies on the interaction among toxin binding, membrane transport, dialysate-side capture, and operating conditions. Therefore, evaluating how different dialyzers perform within an albumin-based detoxification system remains an important step toward improving extracorporeal support technologies for protein-bound toxin removal [30].

1.2.4 Motivation for the Present Study

Conventional dialysis is inherently limited in the removal of strongly protein-bound toxins, because membrane transport is restricted primarily to the unbound solute fraction in circulation [15]. As a result, toxins such as indoxyl sulfate and bilirubin are not efficiently cleared by standard diffusion-based dialysis, despite their important roles in the progression of renal and hepatic dysfunction. This limitation motivates the exploration of alternative extracorporeal detoxification strategies capable of enhancing the removal of albumin-associated solutes.

Albumin dialysis represents one such strategy. By incorporating albumin into the dialysate, it provides additional binding capacity on the dialysate side and thereby helps maintain the concentration gradient required for continued toxin transfer across the membrane. This mechanism makes albumin dialysis particularly attractive for the removal of protein-bound toxins that are otherwise poorly cleared by conventional dialysis. Nevertheless, its overall performance depends not only on toxin binding equilibrium but also on the characteristics of the dialysis membrane itself.

In particular, membrane material may substantially influence toxin transport and albumin retention, both of which are central to the effectiveness of albumin dialysis. A suitable membrane should facilitate toxin removal while preventing excessive albumin leakage, yet the comparative performance of different dialyzer materials under albumin dialysis condi-

tions has not been fully established. Therefore, the present study was undertaken to compare polysulfone and cellulose dialyzers in an in vitro albumin dialysis system, with emphasis on their abilities to remove representative protein-bound toxins while maintaining albumin retention. This work is intended to provide a clearer basis for membrane selection in the development of albumin-based blood purification systems.

1.3 Flow Control Challenges in Dialysis Systems

1.3.1 Importance of Accurate Fluid Control in Dialysis

Precise fluid control is fundamental to the efficacy of any dialysis system. While membrane properties dictate the theoretical limits of solute transport, actual treatment performance relies heavily on the synchronized delivery of multiple fluid streams [31]. Blood, dialysate, and ultrafiltration flow rates must be tightly regulated against their prescribed setpoints to maintain stable clearance [8]. Even minor flow deviations can perturb dialyzer residence times, degrade mass transfer efficiency, and propagate cumulative volumetric errors [32]. Consequently, establishing a robust fluid management architecture is a primary engineering imperative to prevent hemodynamic instability and ensure overall treatment safety [33].

1.3.2 Limitations of Existing Pumping and Control Approaches

Existing pumping and control approaches in dialysis systems are often constrained by a tradeoff between mechanical simplicity and flow regulation accuracy [34]. In many conventional and prototype systems, fluid delivery is achieved using fixed-speed pump operation, where a prescribed rotational speed is assumed to correspond to a desired flow rate. However, this open-loop strategy does not account for variations in tubing compliance, pressure fluctuations, fluid viscosity, pump wear, or changes in hydraulic resistance during treatment [7, 35]. As a result, the actual delivered flow may deviate from the target value even when the pump speed remains constant. These discrepancies become particularly problematic in

dialysis applications, where multiple fluid pathways must operate in a coordinated manner over extended treatment periods [36]. Small instantaneous flow errors can accumulate over time, leading to imbalance between inflow and outflow streams, reduced control over ultrafiltration, and deterioration in overall treatment consistency.

More advanced dialysis platforms may incorporate sensors, balancing chambers, or closed-loop feedback mechanisms to improve volumetric accuracy [37], but such solutions are often associated with increased system complexity, cost, and hardware dependence. These requirements can limit their practicality for compact, portable, or modular dialysis devices, where simplicity, low power consumption, and ease of integration are also critical design objectives. Consequently, existing approaches either lack sufficient adaptability to real-time operating disturbances or rely on complex architectures that are difficult to translate into smaller-scale systems [38]. This limitation highlights the need for a control strategy that can maintain accurate and stable flow delivery while remaining compatible with compact and automated dialysis platforms [39].

1.3.3 Motivation for the Present Flow Control Study

Precise flow regulation is a fundamental requirement in extracorporeal blood purification systems, because treatment performance depends directly on the accurate delivery and balance of circulating fluids. In practical operation, however, many dialysis-related pumping systems are still run primarily at fixed motor speeds, with the expectation that a constant rotational speed will produce a constant flow rate. This assumption is not always valid. The actual delivered flow can vary over time as a result of tubing compliance, hydraulic resistance, pressure fluctuations, pump loading, and other system-level disturbances. Consequently, fixed-speed operation may lead to appreciable flow instability and cumulative volumetric error, even when the nominal pump setting remains unchanged [7, 35, 36].

These limitations are particularly important in the context of a portable and fully automated artificial kidney system. Compared with conventional stationary clinical platforms, such a system must operate with a higher degree of autonomy and reliability while maintain-

ing tight control over fluid transport. Under these conditions, inaccurate flow delivery is not merely a minor operational deviation; it can affect treatment consistency, compromise fluid management, and reduce confidence in the overall performance of the device. Therefore, achieving stable and accurate flow is a central engineering challenge in the development of compact automated extracorporeal systems [38, 40].

The present flow control study was motivated by this need to move beyond open-loop fixed-speed pumping and toward a more reliable method of flow regulation. Specifically, it was necessary to evaluate whether feedback-based control could reduce fluctuations in the actual flow rate and improve agreement between intended and delivered volume over extended operation. By characterizing flow stability and volumetric accuracy under controlled experimental conditions, this study aims to provide the engineering basis for more precise fluid management in next-generation artificial kidney platforms.

1.4 Portable Dialysis Machine Design

1.4.1 Current Limitations and Clinical Challenges

Conventional dialysis systems are generally developed for fixed clinical or home-based use and often rely on substantial supporting infrastructure, which limits their portability and flexibility of deployment [38]. In recent years, increasing interest in portable, wearable, and implantable artificial kidney systems has further highlighted the need for more compact and mobile dialysis technologies [41].

In addition to their physical size, current dialysis systems also require multiple setup procedures before treatment, including circuit priming, tubing installation, and connection of the extracorporeal flow path. These procedures are safety-critical and operationally demanding. Clinical guidance has emphasized that incorrect connection or disconnection of a patient from the extracorporeal circuit can lead to complications, particularly when staff are working under procedural time pressure [42, 43]. Human-factors evaluations of newer dialysis systems have similarly shown that usability and safety are important design considerations

for improving operation and reducing barriers to broader adoption [44].

Therefore, the design of a portable dialysis machine should not focus solely on miniaturization. It should also simplify system setup, reduce operator burden, and improve the reliability of flow delivery and circuit assembly. These considerations are especially important for systems intended to move beyond conventional large-scale machine architectures toward more portable and user-friendly platforms [41].

Motivated by these limitations, the present study adopts a compact machine architecture aimed at improving portability, a combined pump configuration to enhance flow-rate accuracy, and a cassette-based design intended to reduce tubing installation errors and improve operational reliability.

1.4.2 Compact System Architecture

A portable dialysis machine requires a compact and integrated architecture rather than the large and infrastructure-dependent layouts commonly used in conventional systems [41]. In this study, the system was designed as a compact platform that consolidates key functional modules within a reduced footprint. This architectural approach is intended to improve portability and to provide a foundation for reliable flow regulation and simplified circuit setup, while detailed hardware implementation is presented in later chapters.

1.4.3 Flow Accuracy and Operational Reliability

In addition to compactness, a portable dialysis machine must provide accurate flow delivery and reliable operation. Flow accuracy is essential for maintaining stable and predictable system performance, while operational reliability is necessary not only during treatment, but also during circuit setup and machine preparation [41]. For portable applications, these requirements become especially important because system miniaturization should not come at the cost of reduced performance or increased operator burden [38].

Motivated by these considerations, the present study employs a combined pump configuration to improve flow-rate accuracy and a cassette-based design to simplify circuit setup

and reduce the likelihood of tubing installation errors. The detailed design rationale and experimental evaluation are presented in later chapters.

1.5 Research Objectives and Scope

This thesis focuses on three closely related aspects of artificial kidney development: albumin dialysis for protein-bound toxin removal, flow control for accurate fluid delivery, and the design and performance evaluation of a new portable machine. Together, these studies aim to advance the engineering development of a compact and automated extracorporeal blood purification platform.

The first objective of this work is to investigate albumin dialysis as a strategy for removing representative protein-bound toxins. Conventional dialysis is limited in its ability to remove strongly albumin-bound solutes, whereas albumin dialysis can improve their transfer by providing binding capacity on the dialysate side. In this thesis, albumin dialysis is studied under controlled in vitro conditions, with particular emphasis on comparing polysulfone and cellulose dialyzers. The aim is to determine how membrane material influences toxin removal behavior and albumin retention, both of which are critical to the effectiveness of albumin-based extracorporeal detoxification.

The second objective is to evaluate flow control performance in the artificial kidney system. Accurate and stable flow delivery is essential for reliable extracorporeal operation, since deviations in the actual flow rate can affect treatment consistency and cumulative volumetric accuracy. This part of the study therefore examines the ability of the system to maintain the intended flow under defined operating conditions. The aim is to assess flow stability and flow accuracy as key indicators of engineering performance in the developed platform.

The third objective is to design and develop a new portable artificial kidney machine and evaluate its overall performance as an integrated prototype. This includes the implementation of a new system design, a cassette-based configuration, and a pump arrangement combining large and small pumps to meet different fluid-handling requirements within the

circuit. The aim of this part of the work is not only to establish a more compact and practical prototype architecture, but also to determine whether the resulting machine can provide the operational performance required for artificial kidney applications.

The scope of this thesis is limited to benchtop in vitro studies performed on the developed prototype platform. The work focuses on engineering feasibility, membrane-dependent dialysis performance, and system-level operational behavior. It does not include clinical validation, in vivo testing, long-term biocompatibility assessment, or full optimization of all hardware and control subsystems. Instead, the thesis is confined to three specific areas: albumin dialysis performance, flow control capability, and the design and performance evaluation of a new portable machine.

Taken together, these objectives define the research framework of the present study. By addressing detoxification performance, fluid regulation, and prototype development within a single artificial kidney platform, this thesis seeks to provide a clearer engineering basis for future improvements in portable and automated blood purification systems.

1.6 Organization of the Thesis

This thesis is organized into four main chapters. Chapter 1 introduces the background and motivation of the study, including the limitations of conventional dialysis, the need for improved protein-bound toxin removal, the importance of accurate fluid control, and the design challenges associated with portable dialysis systems. The research objectives and scope of the thesis are also defined in this chapter.

Chapter 2 presents the albumin dialysis study. It describes the preparation of dialysate and albumin solutions, the experimental setup, and the evaluation of polysulfone and cellulose dialyzers for the removal of representative protein-bound toxins. The chapter also discusses the measured changes in indoxyl sulfate, bilirubin, and bovine serum albumin concentrations during the 3-hour in vitro dialysis experiments.

Chapter 3 focuses on PI flow-control development. It introduces the pump calibration procedure, the implementation of closed-loop proportional-integral control, and the TV-

MTLSTM-based procedure used to predict optimized channel-specific PI gains. Different controller settings are compared to assess their effects on flow response and cumulative error.

Chapter 4 describes the design and integration of the portable dialysis platform. It presents the overall system architecture, prototype fabrication, cassette-based layout, electrical and control integration, and bubble-detection-based safety mechanism. The chapter also evaluates the representative system-level performance of the developed prototype.

Chapter 2
ALBUMIN DIALYSIS

2.1 Preparation of Dialysate and Albumin Solutions

For the albumin dialysis experiments, both the dialysate and albumin-containing solutions were prepared prior to each run.

2.1.1 Dialysate preparation

A total of 3 L of dialysate was prepared according to the manufacturer's instructions. The required amounts of Solution A and Solution B were first calculated based on the recommended mixing ratio. Deionized (DI) water was added to the container first, followed by Solution A and Solution B. The mixture was then gently stirred until a homogeneous dialysate solution was obtained.

2.1.2 Albumin solution preparation

Two clean 2 L beakers were prepared for the albumin solutions. One solution was used as the blood-side solution and the other as the dialysate-side solution. The blood-side solution was prepared to a final volume of 500 mL with an albumin concentration of 3.5 g/dL, while the dialysate-side solution was prepared to a final volume of 500 mL with an albumin concentration of 4.0 g/dL.

For each solution, the required amount of albumin powder was added into the beaker, and a magnetic stir bar was placed inside. The beaker was weighed and the initial mass was recorded. Approximately 300 mL of prepared dialysate was then added, and the solution was stirred continuously until the albumin was completely dissolved. After dissolution, the solution was slowly transferred to a graduated cylinder or volumetric flask and brought

to a final volume of 500 mL with dialysate. Since substantial foam formed during the preparation process, all transfers were performed slowly to minimize foaming and reduce volume measurement error.

2.1.3 Toxin spiking

After preparation of the albumin solution, 495 mL of the blood-side solution was transferred into the blood beaker. Indoxyl sulfate and bilirubin were then added to the blood-side solution as the two representative protein-bound toxins.

To prepare a final indoxyl sulfate concentration of 3 mg/dL, 750 μL of a 20 mg/mL indoxyl sulfate potassium stock solution was added to the blood-side solution and mixed thoroughly.

To prepare a final bilirubin concentration of 20 mg/dL, 5 mL of a 20 mg/mL bilirubin stock solution was added to the blood-side solution and mixed thoroughly.

2.2 Experiment

Albumin dialysis experiments were conducted to evaluate the performance of the portable dialysis platform over a 3 h treatment period. Two different dialyzer membrane materials, polysulfone and cellulose, were investigated to compare their performance in the removal of representative protein-bound toxins under the same operating conditions.

As shown in Figure 2.1, for each experiment, the prepared blood-side solution and albumin-containing dialysate were introduced into the system after circuit assembly and priming had been completed. Albumin dialysis was then performed for 3 h. During each run, the blood-side solution and the albumin dialysate circulated on opposite sides of the dialyzer, with both flow rates maintained at 180 mL/min throughout the experiment.

Samples were collected from both the blood-side reservoir and the albumin dialysate reservoir at 0, 0.5, 1, 2, and 3 h. These samples were used to quantify toxin transport and evaluate dialysis performance as a function of time. Indoxyl sulfate concentration was measured using an isotope-labeling method, while bilirubin and bovine serum albumin (BSA)

concentrations were measured using mass spectrometry. Measurement of BSA was also used to evaluate albumin retention during dialysis.

For each membrane type, three independent replicate experiments were performed. The resulting data were used to compare the dialysis performance of the polysulfone and cellulose dialyzers over the 3 h treatment period.

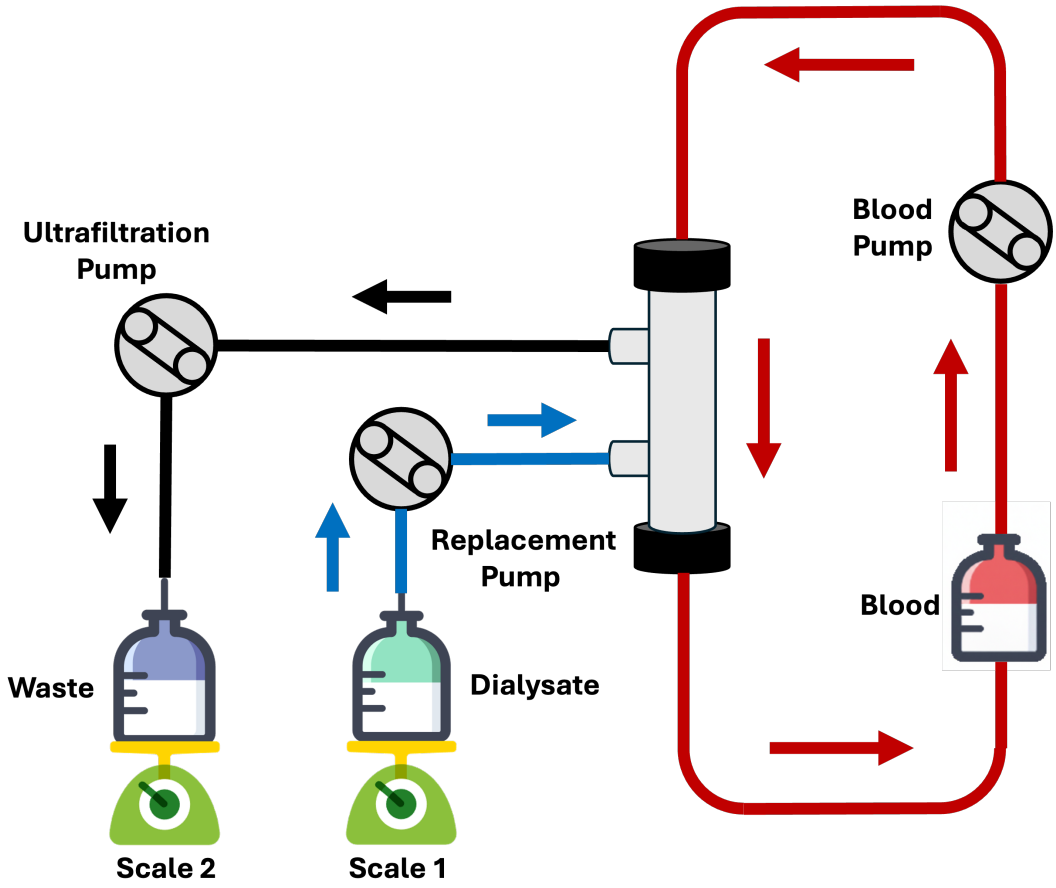

Figure 2.1: Schematic of the albumin dialysis setup showing the blood-side solution loop and the albumin-containing dialysate loop across the dialyzer.

2.3 Results

2.3.1 Results for Indoxyl Sulfate

To evaluate the clearance performance of different dialyzer membranes, the concentration of indoxyl sulfate (IS), a representative protein-bound uremic toxin, was monitored on the blood side over a 3-hour in vitro dialysis experiment. As shown in Figure 2.2, most membrane trials exhibited a rapid initial decrease in blood-side IS concentration within the first 0.5 h, indicating fast toxin transfer driven by the large initial concentration gradient across the membrane. After this initial phase, the rate of concentration change became markedly smaller, and the measured concentrations generally approached a quasi-steady level over the remainder of the experiment. In contrast, the Cellulose Control group maintained the highest residual IS concentration throughout the experiment and showed only a modest overall decline, consistent with its role as the control condition. A temporary increase was observed in Cellulose T1 at $t = 2$ h, which may be attributed to sampling variability or a minor transient disturbance in the closed-loop system.

As an aggregate measure of clearance performance, the blood-side concentration of indoxyl sulfate (IS) was averaged across multiple trials for the Cellulose and Polysulfone dialyzer membranes, and the results are presented as mean $\pm$ standard deviation in Figure 2.3. Both membrane groups showed a pronounced reduction in IS concentration during the first 0.5 h, consistent with rapid initial toxin transfer driven by the large concentration gradient across the membrane. After this initial decline, the mean concentrations changed only modestly from 0.5 to 3 h, indicating an approach toward a quasi-steady level over the remainder of the experiment. The mean concentration profiles of the Cellulose and Polysulfone groups remained broadly similar throughout the study, suggesting comparable overall IS removal behavior under the tested conditions. The relatively large standard deviations during the later stage reflect trial-to-trial variability in the measured concentrations.

For endpoint interpretation, the IS results were compared with reported uremic concentration levels. A review of uremic toxin concentrations reported a mean uremic total IS

concentration of approximately 23.1 mg/L, or 2.31 mg/dL [45]. In the present experiments, the mean blood-side IS concentration decreased from approximately 2.8–2.9 mg/dL at baseline to 1.44 mg/dL for the Cellulose group and 1.41 mg/dL for the Polysulfone group after 3 h. Both endpoint concentrations were below the reference uremic level and therefore fell within the safe range used for interpreting the experimental results. These findings indicate that both dialyzer membranes reduced IS to an acceptable endpoint level under the tested conditions.

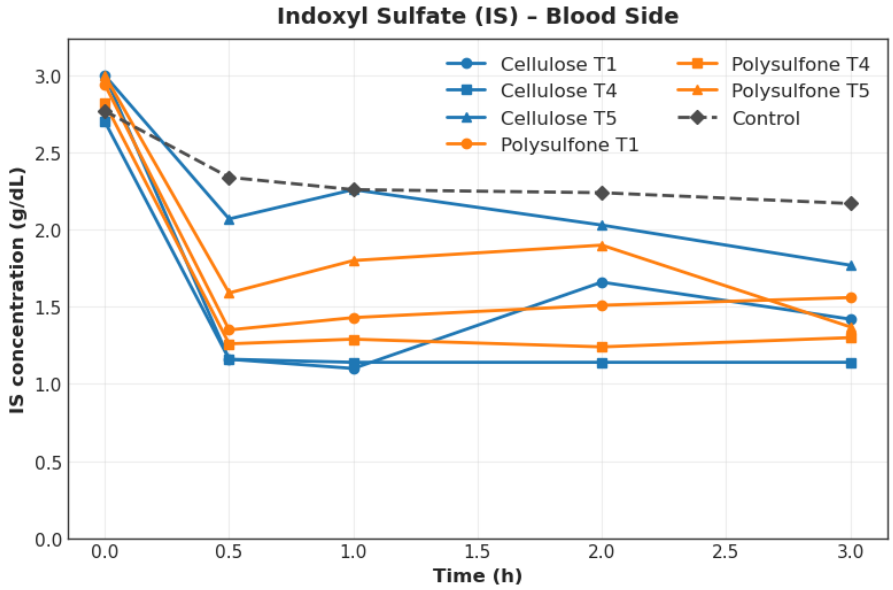

Figure 2.2: Blood-side indoxyl sulfate (IS) concentration during the 3-hour in vitro dialysis experiment.

To complement the blood-side concentration measurements, the accumulation of indoxyl sulfate (IS) on the dialysate side was monitored over the same 3-hour in vitro dialysis experiment. As shown in Figure 2.4, most membrane trials exhibited a rapid increase in dialysate-side IS concentration during the first 0.5 h, consistent with fast toxin transfer from the blood side under the initial transmembrane concentration gradient. After this initial rise, the dialysate concentrations changed more gradually over the remainder of the experiment

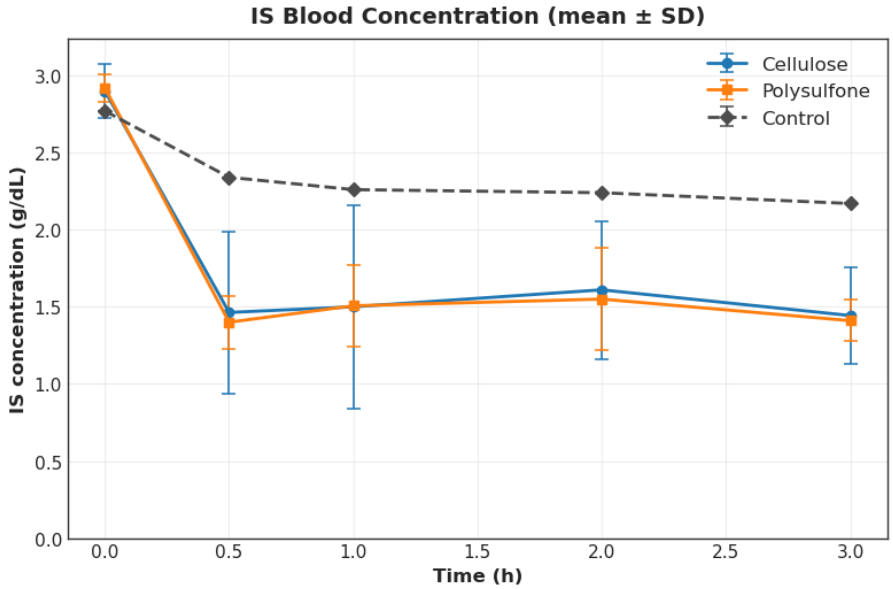

Figure 2.3: Mean blood-side indoxyl sulfate (IS) concentration during the 3-hour in vitro dialysis experiment. Data are shown as mean ± standard deviation.

and generally remained within a relatively narrow range, although modest fluctuations were observed in several trials at later time points. In contrast, the Cellulose Control trial showed only minimal IS accumulation throughout the experiment, consistent with its role as the control condition. Overall, the dialysate-side profiles were qualitatively consistent with the corresponding decrease in blood-side IS concentration.

As an aggregate measure of indoxyl sulfate (IS) transfer into the dialysate compartment, dialysate-side concentration data were averaged across multiple trials for the Cellulose and Polysulfone dialyzer membranes, and the results are presented as mean ± standard deviation in Figure 2.5. Both membrane groups showed a pronounced increase in dialysate-side IS concentration during the first 0.5 h, consistent with rapid initial toxin transfer from the blood side under the large transmembrane concentration gradient. After this initial rise, the mean concentrations changed only modestly from 0.5 to 3 h, indicating an approach toward a quasi-steady level over the remainder of the experiment. The mean dialysate-

side concentration profiles of the Cellulose and Polysulfone groups remained broadly similar throughout the study, suggesting comparable overall IS transfer behavior under the tested conditions. The relatively large standard deviations at later time points reflect trial-to-trial variability in the measured concentrations.

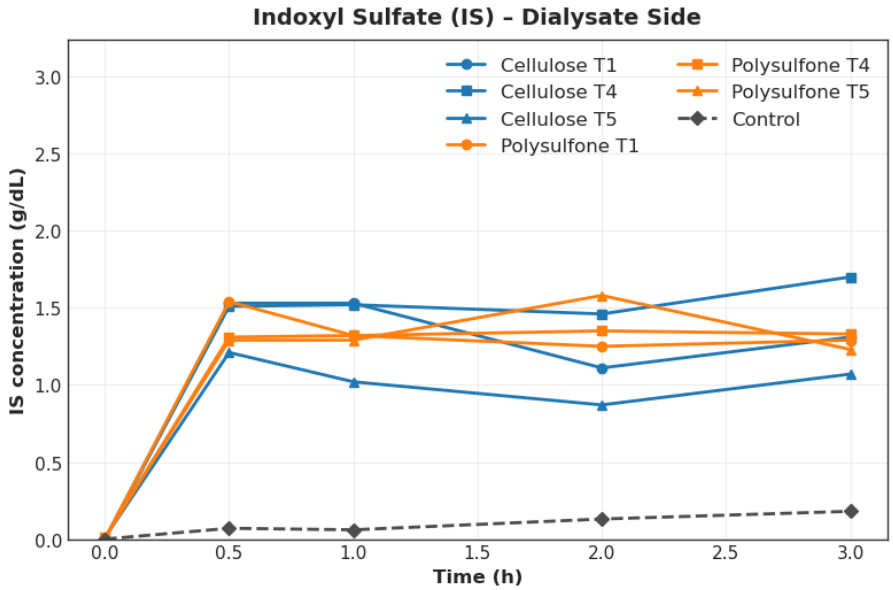

Figure 2.4: Time-course profile of indoxyl sulfate (IS) concentration on the dialysate side during a 3-hour in vitro dialysis experiment.

2.3.2 Results for Bilirubin

To evaluate the removal of bilirubin, a larger and strongly protein-bound toxin, the blood-side bilirubin concentration was monitored over a 3-hour in vitro experiment. As shown in Figure 2.6, bilirubin concentration decreased progressively in all membrane trials throughout the experiment. In contrast to the rapid early change observed for indoxyl sulfate, the decline in bilirubin was sustained over the full 3-hour period, suggesting a more gradual transfer process. Among the tested membranes, the Polysulfone trials generally exhibited lower blood-side bilirubin concentrations at later time points than the Cellulose trials,

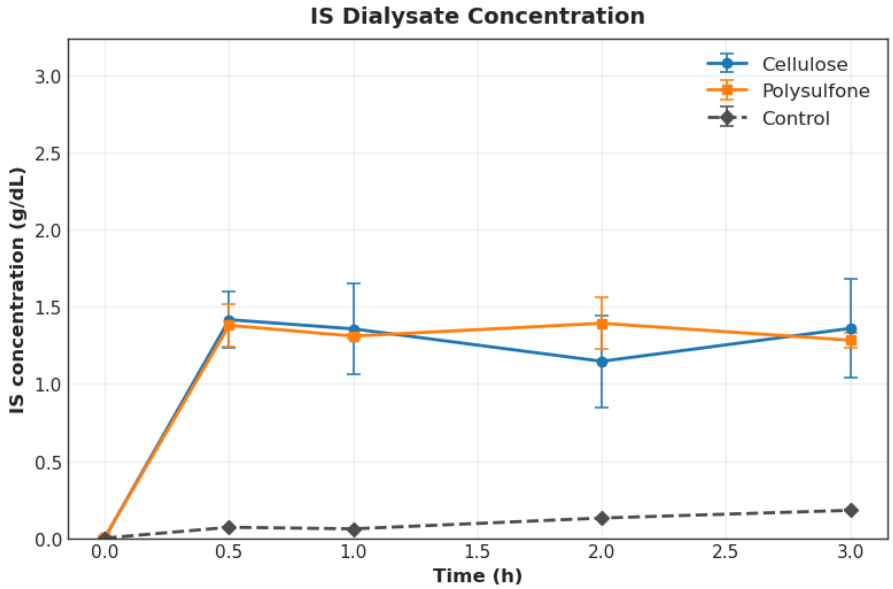

Figure 2.5: Mean dialysate-side concentration profiles of indoxyl sulfate (IS) during a 3-hour in vitro dialysis experiment.

indicating better overall bilirubin removal under the tested conditions. In comparison, the Cellulose Control showed only a slight decline and remained at a relatively high concentration level throughout the experiment, consistent with its role as the control condition.

The replicate-averaged bilirubin results are shown in Figure 2.7. The mean blood-side bilirubin concentration decreased from approximately 18 mg/dL at baseline to approximately 10.8 mg/dL for the Cellulose group and 8.8 mg/dL for the Polysulfone group after 3 h. These results show meaningful bilirubin reduction over the treatment period, with the Polysulfone group reaching a lower endpoint concentration than the Cellulose group.

To complement the blood-side bilirubin measurements, the accumulation of bilirubin on the dialysate side was monitored over the same 3-hour in vitro experiment. As shown in Figure 2.8, bilirubin concentration increased progressively in all membrane trials throughout the experiment. The dialysate-side profiles were qualitatively consistent with the corresponding decrease in blood-side bilirubin concentration, reflecting continued transfer of bilirubin

across the membrane over time. Compared with the Cellulose trials, the Polysulfone trials generally showed higher dialysate-side bilirubin concentrations and a faster overall rise, indicating better overall bilirubin transfer under the tested conditions. In contrast, the Cellulose Control remained near baseline throughout the experiment, consistent with its role as the control condition. The mean ± standard deviation dialysate-side results in Figure 2.9 further support this trend, with the Polysulfone group showing greater bilirubin accumulation in the dialysate by the end of treatment.

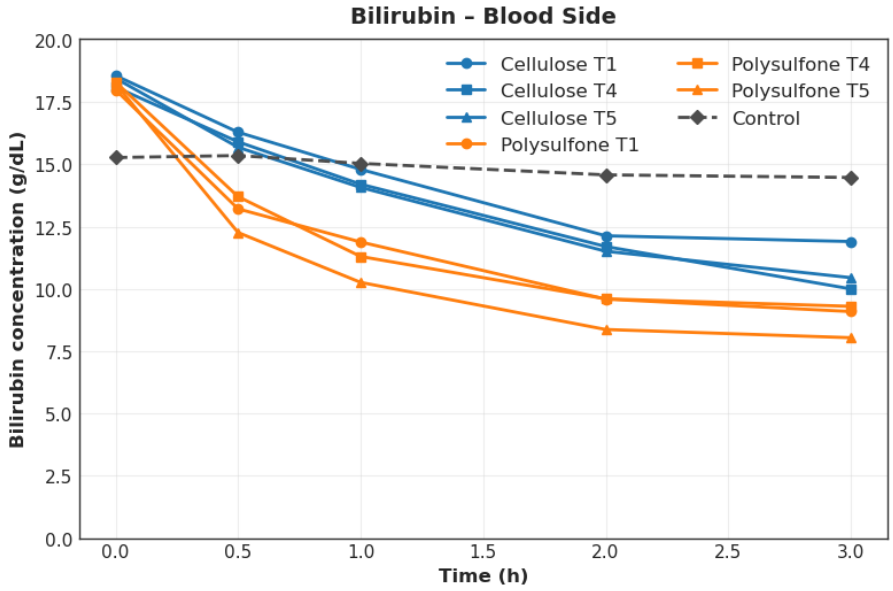

Figure 2.6: Time-course profile of blood-side bilirubin concentration during a 3-hour in vitro dialysis experiment.

2.3.3 Results for Bovine Serum Albumin

To evaluate the protein retention performance of the dialyzer membranes, the blood-side concentration of bovine serum albumin (BSA) was monitored over a 3-hour in vitro experiment. As shown in Figure 2.10, the BSA concentration remained within a relatively narrow range in all trials throughout the experiment and did not exhibit a clear downward

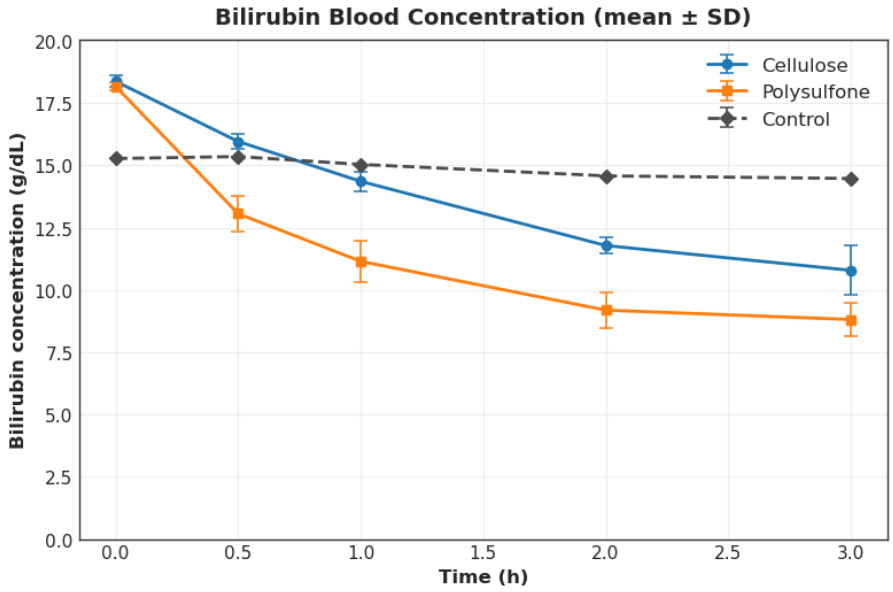

Figure 2.7: Mean blood-side bilirubin concentration during the 3-hour in vitro dialysis experiment. Data are shown as mean ± standard deviation.

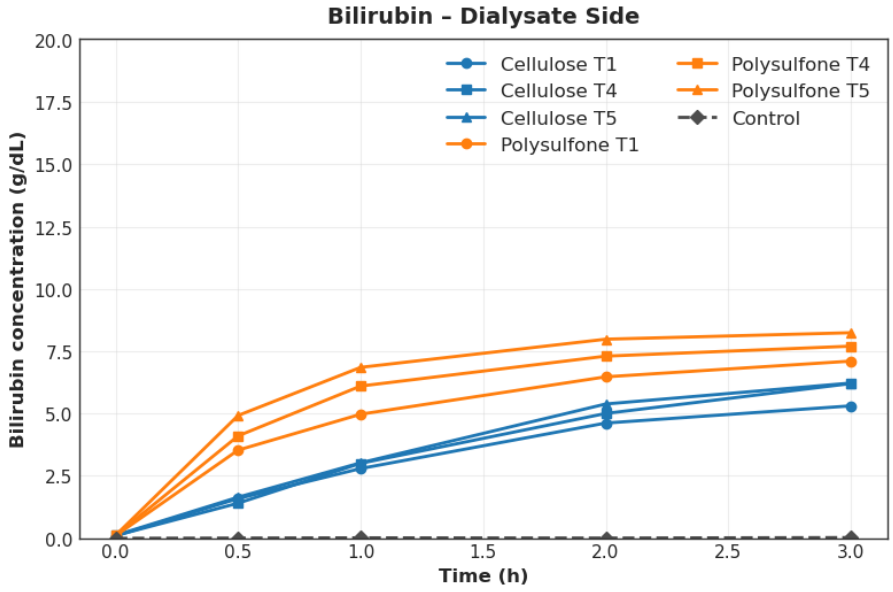

Figure 2.8: Time-course profile of dialysate-side bilirubin concentration during a 3-hour in vitro dialysis experiment.

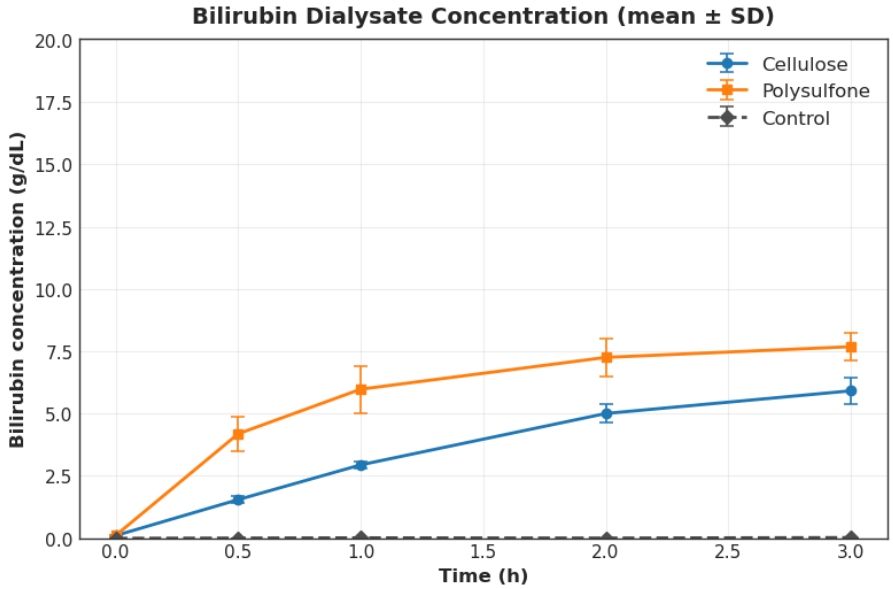

Figure 2.9: Mean dialysate-side bilirubin concentration during the 3-hour in vitro dialysis experiment. Data are shown as mean ± standard deviation.

trend. This overall stability suggests that both the Cellulose and Polysulfone membranes retained BSA effectively under the tested conditions, with minimal transmembrane protein loss. Although minor fluctuations were observed at several time points, such as the temporary increase in Cellulose T1 at $t = 2$ h, the blood-side BSA concentration remained generally stable over the full experimental period. The Cellulose Control also showed only a slight overall change, consistent with a stable baseline condition. The mean ± standard deviation results in Figure 2.11 show the same general pattern and indicate that variability did not correspond to a systematic loss of blood-side albumin.

To assess the stability of bovine serum albumin (BSA) in the dialysate compartment, the dialysate-side BSA concentration was monitored over a 3-hour in vitro experiment. As shown in Figure 2.12, the dialysate-side BSA concentration in all membrane trials remained within a relatively narrow range throughout the experiment, with no clear increasing or decreasing trend over time. This result indicates that the BSA-containing dialysate main-

tained a generally stable albumin level under the tested conditions. In contrast, the Cellulose Control remained near zero throughout the experiment because the control dialysate did not contain BSA. Although minor fluctuations were observed among individual membrane trials, the dialysate-side BSA concentration was generally stable over the full experimental period. The averaged results in Figure 2.13 confirm that neither membrane group showed progressive depletion of dialysate-side albumin during the experiment.

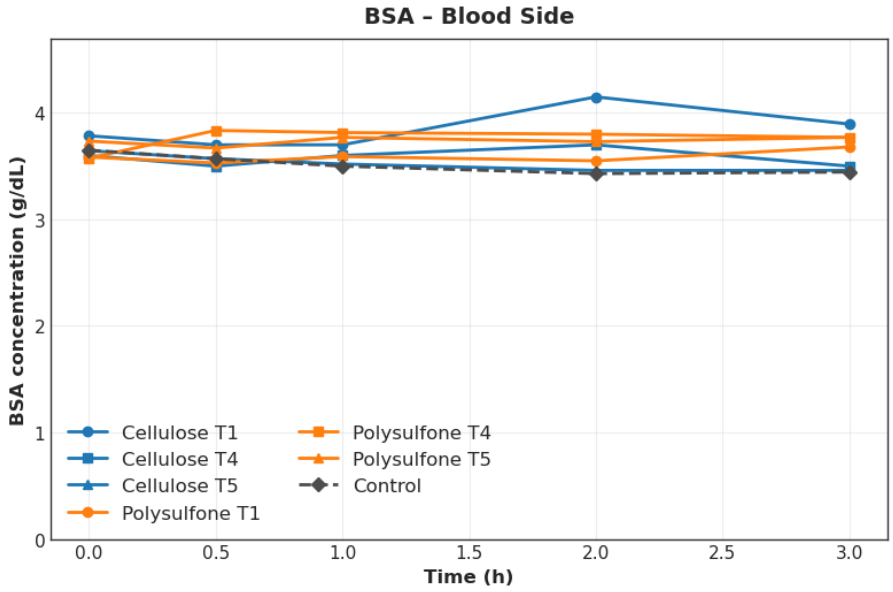

Figure 2.10: Time-course profile of blood-side bovine serum albumin (BSA) concentration during a 3-hour in vitro dialysis experiment.

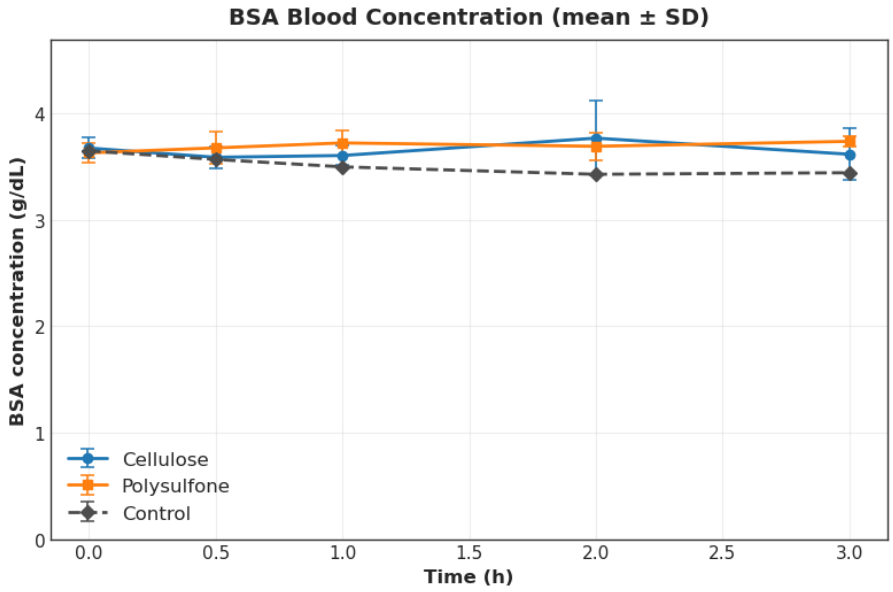

Figure 2.11: Mean blood-side bovine serum albumin (BSA) concentration during the 3-hour in vitro dialysis experiment. Data are shown as mean ± standard deviation.

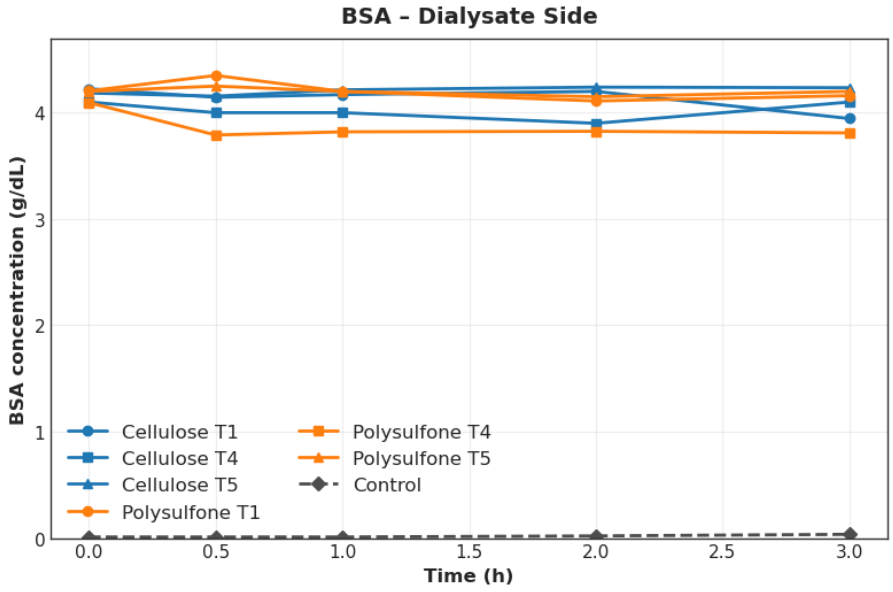

Figure 2.12: Time-course profile of dialysate-side bovine serum albumin (BSA) concentration during a 3-hour in vitro dialysis experiment.

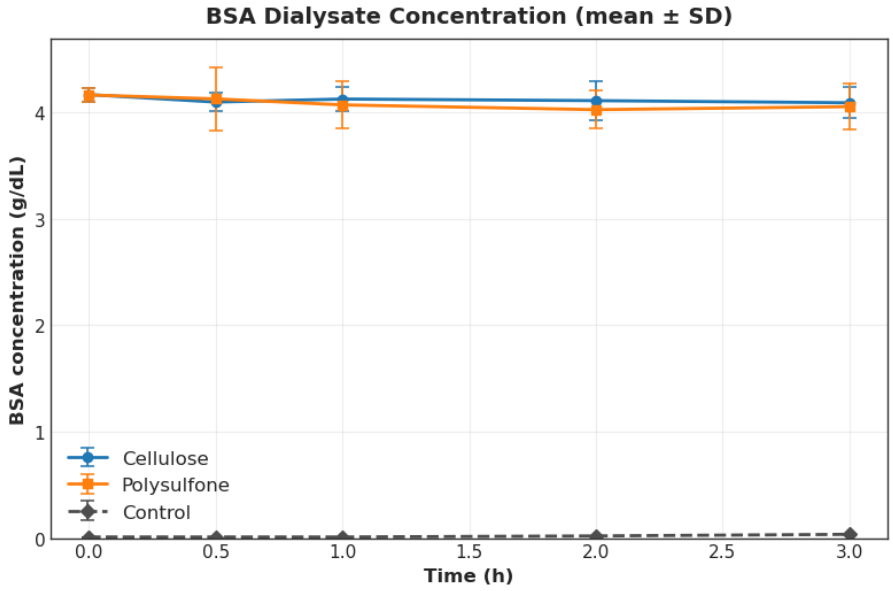

Figure 2.13: Mean dialysate-side bovine serum albumin (BSA) concentration during the 3-hour in vitro dialysis experiment. Data are shown as mean ± standard deviation.

Chapter 3

PI FLOW CONTROL DEVELOPMENT

3.1 Hemofiltration System Setup

The experimental platform used for flow-control validation was a custom benchtop pre-dilution hemofiltration (HF) circuit (Figure 3.1). It comprised a blood loop, a replacement fluid supply path, and an ultrafiltration path. The replacement pump (RP) drew fluid from the replacement fluid reservoir and infused it into the hemofilter. The ultrafiltration pump (UF) drew waste fluid into the waste reservoir. Scale 1, placed beneath the replacement fluid reservoir, and Scale 2, placed beneath the waste reservoir, continuously recorded mass changes. Under the water-density assumption of 1 g/mL, these measurements were used to calculate the instantaneous RP and UF volumetric flow rates in real time.

The platform was operated exclusively in the pre-dilution HF configuration for all PI-control experiments reported in this thesis. Post-dilution and hemodiafiltration modes, as well as comparisons between dilution modes, were outside the scope of the flow-control study. This experimental definition is consistent with the Scientific Reports manuscript and avoids interpreting the PI-control results as dilution-mode comparisons.

3.2 Pump Calibration

Accurate control of flow in the extracorporeal platform requires a precise mapping between peristaltic-pump speed and volumetric output, since flow rate is determined by the tubing inner diameter and elasticity. PharMed silicone tubing with dimensions of 4.8 mm $\times$ 8 mm was evaluated by operating each pump at several fixed speeds and measuring the effluent volume over repeated 60 s intervals using scales with $\pm 0.5\%$ accuracy. During calibration, each pump was driven at incrementally increasing speeds from 10 to 100 rpm. At each set-

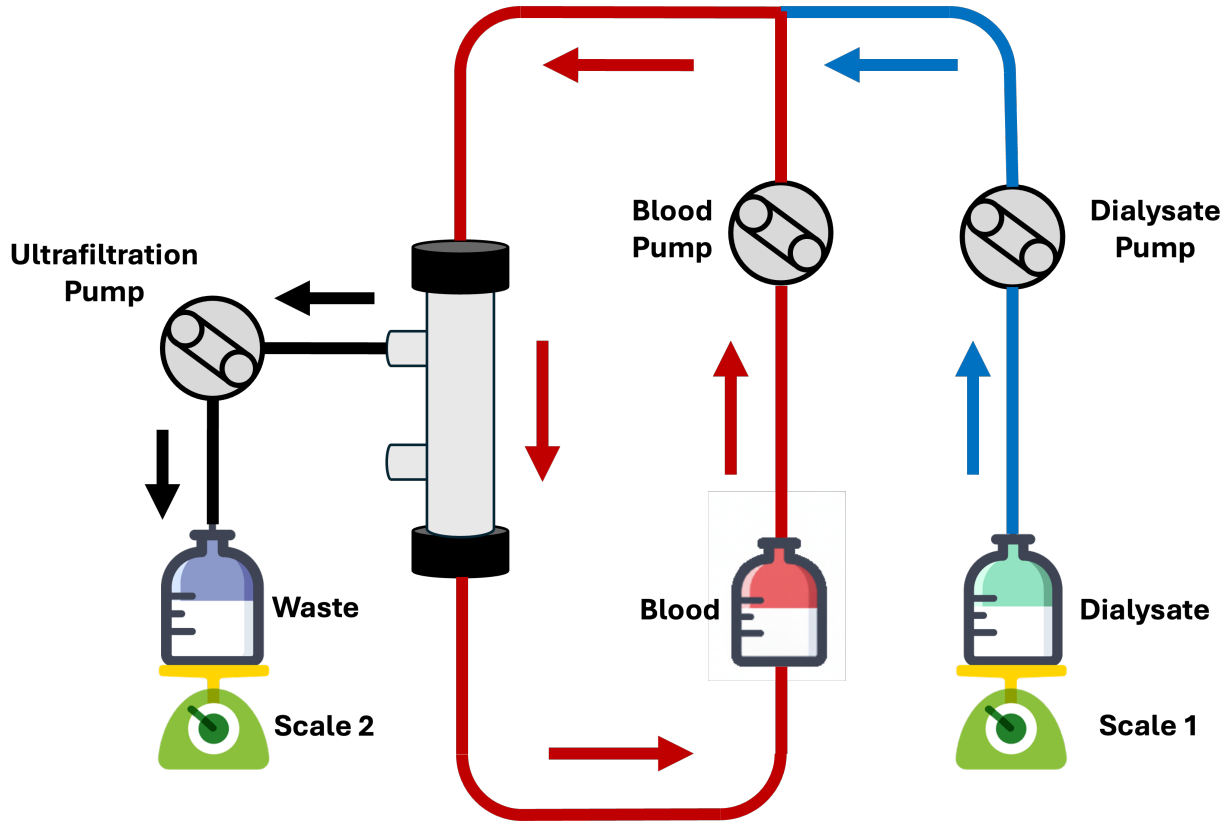

Figure 3.1: Schematic of the benchtop pre-dilution hemofiltration circuit. The red line represents the blood loop; the blue line represents the replacement fluid supply and ultrafiltration path. Scale 1, located beneath the replacement fluid reservoir, and Scale 2, located beneath the waste reservoir, continuously record mass changes, from which the RP and UF volumetric flow rates are derived in real time. The platform is fixed in the pre-dilution configuration for the flow-control experiments.

point, the steady-state flow was recorded three times and averaged. A least-squares fit of flow rate in mL/min to rotational speed in rpm yielded negligible intercepts (< 0.1 mL/min) and highly consistent slopes across pumps, with variation below 3%. The tubing showed excellent linearity during speed ramps, with $R^2 > 0.995$.

$$Q\,[\text{mL/min}] = k \cdot \text{rotational speed (rpm)}, \qquad k = 0.58 \tag{3.1}$$

where Q is the pump flow rate. The calibration coefficient $k = 0.58$ represents the combined effects of tubing geometry and material properties on the relationship between pump speed and flow rate.

To enable seamless integration with the PI control algorithm, the calibration constant was stored in a dictionary at initialization. During closed-loop operation, the controller converted the desired flow setpoint into the corresponding rpm command through this lookup, and then compared feedback-derived flow measurements with the target value to compute the PI error. By grounding the control logic in experimentally derived calibration data, the system achieved flow tracking close to the target under nominal conditions despite tubing compliance and fluid-viscosity variations.

3.3 PI Feedback Control of the Peristaltic Pumps

A proportional–integral (PI) control algorithm was implemented for the replacement and ultrafiltration pumps. Unlike traditional open-loop control, which relies on fixed motor speeds and is susceptible to mechanical variations and changes in fluid properties, PI control provides real-time correction driven by feedback.

The proportional component reacts to the current error between the desired and actual flow rates and provides immediate corrective action. The integral component accumulates past errors over time, which ensures that steady-state deviations are eliminated. By combining these two effects, PI control maintains flow stability within tight tolerance bounds, which improves both treatment safety and patient comfort.

In conventional clinical settings, peristaltic pumps used in hemofiltration devices often operate under open-loop control, where the rotational speed of each pump is manually set and held constant throughout treatment. This approach is simple to implement but fails to compensate for system-level variations such as tubing elasticity, fluid-viscosity changes, and mechanical tolerances.

To investigate the limitations of fixed-speed operation, benchtop experiments were conducted on both the UF and RP pumps, with each pump operated at a constant rpm corresponding to a nominal target flow of 40 mL/min. The results are shown in Figure 4.2. Despite the fixed input, the two channels exhibited persistent deviations from the target flow rather than converging to the nominal setpoint. The RP flow remained above the target, ranging from 43.80 to 45.89 mL/min, whereas the UF flow remained below the target, ranging from 31.18 to 35.06 mL/min. Over the 60-min experiment, these channel-dependent offsets produced substantial cumulative-volume drift. The maximum absolute cumulative errors reached 289.77 mL for the RP channel and 339.20 mL for the UF channel, respectively.

The two channels exhibited different error characteristics, reflecting the sensitivity of flow performance to hydraulic boundary conditions and system geometry. A likely explanation is the physical configuration of the fluid pathways. In this setup, the UF tubing is suspended and its outlet faces minimal resistance during drainage, which allows relatively stable outflow. In contrast, the RP channel draws fluid from a submerged inlet, where hydrostatic pressure and fluid interactions may vary over time due to transient dynamics such as tubing compression, backflow resistance, or minor pressure build-up. These factors can introduce flow disturbances even when the pump speed is held constant. While the exact mechanism is not fully understood, this asymmetry highlights the sensitivity of flow performance to hydraulic boundary conditions and system geometry.

These findings illustrate the inherent inaccuracy of open-loop pump control, where neither moment-to-moment flow consistency nor long-term volumetric accuracy can be guaranteed. In a clinical setting, such discrepancies could cause improper fluid balance, patient discomfort, or safety risks during prolonged treatment. These issues motivated the transition

to the closed-loop PI control strategy discussed below.

To address the limitations of open-loop control, a closed-loop flow-regulation system based on a PI controller was developed and implemented. At fixed time intervals, the system acquires real-time flow measurements from an integrated scale module, which provides both instantaneous and accumulated mass-transfer data. Based on this feedback, the controller calculates a corrective adjustment to the flow rate in mL/min as

$$\Delta Q_k = K_p \left(Q^* - Q_k\right) + K_i \sum_{i=0}^{k} \left(Q^* - Q_i\right) \Delta t \tag{3.2}$$

where Q^* is the target flow rate, Q_k is the measured instantaneous flow rate, and the summation represents the discrete integral of past flow errors. The constants K_p and K_i are controller gains tuned to balance responsiveness and stability.

This adjustment is then applied to update the flow-rate estimate for the next control interval,

$$Q_{k+1} = Q_k + \Delta Q_k \tag{3.3}$$

To implement this change at the hardware level, the updated flow rate is converted into a corresponding pump speed in rpm using the pre-calibrated linear relationship derived from benchtop testing,

$$\mathrm{RPM}_{k+1} = \frac{Q_{k+1}}{k} \tag{3.4}$$

where k is the calibration coefficient determined experimentally during the initial pump-calibration stage with the selected yellow tubing (Equation (3.1)). This linear relationship was derived by correlating measured flow rates with pump speeds across a range of operating conditions. By leveraging this conversion, the closed-loop mechanism dynamically adjusts pump speed in response to flow disturbances that arise from variable backpressure, tubing compliance, and mechanical tolerances. As a result, the system achieves substantial improvements in both real-time consistency and long-term volumetric accuracy of fluid delivery.

3.4 Selection of Optimized PI Gains

The optimized PI gains used in the flow-control experiments were obtained through a data-driven gain-prediction procedure rather than by manual trial-and-error selection. A total of 25 fixed-gain PI configurations were tested for each channel on the benchtop pre-dilution hemofiltration platform. Each experimental run generated a time-series record of the measured flow response and cumulative volume behavior under a known gain pair (K_p, K_i). These fixed-gain records provided the training and evaluation data used to learn how different PI settings affected flow stability, transient response, and cumulative-error drift.

For each pump channel, the time-dependent model input included four dynamic features: the measured flow rate $y(t)$, the instantaneous flow error $e(t) = Q^* - y(t)$, the first-order error difference $\Delta e(t)$, and the accumulated flow error $I(t)$. The target flow rate Q^*, fixed at 40 mL/min under the water-density assumption, was included as a static input. Separate models were trained for the replacement pump (RP) and ultrafiltration pump (UF), allowing the two channels to learn different gain responses consistent with their different hydraulic boundary conditions.

The gain-prediction model was a total-variation-regularized multi-head long short-term memory network (TV-MTLSTM). The model first extracted local temporal features from the input sequence, then used stacked LSTM layers to learn longer-term flow-response behavior. The shared temporal representation was connected to two output heads. The main output head predicted the PI gains,

$$\hat{\theta} = (\hat{K}_p, \hat{K}_i), \tag{3.5}$$

while an auxiliary output head predicted the future accumulated-error sequence. This auxiliary task was included because cumulative error is the quantity most directly related to long-term volumetric imbalance in dialysis operation. By requiring the model to predict not only the gain pair but also the future accumulated-error trajectory, the model was encouraged to learn gain settings that improved both instantaneous tracking and long-term

volume control.

Training used a composite loss function combining four terms:

$$L = \lambda_1 L_{\mathrm{PI}} + \lambda_2 L_{\mathrm{seq}} + \lambda_3 L_{\mathrm{TV}} + \lambda_4 L_{\mathrm{term}}. \tag{3.6}$$

Here, L_{PI} penalizes error in the predicted PI gains, L_{seq} penalizes error in the predicted accumulated-error sequence, L_{TV} penalizes abrupt variation in that predicted sequence, and L_{term} penalizes residual accumulated error at the end of the prediction window. The total-variation term was included to discourage oscillatory behavior, while the terminal-error term prevented the model from favoring smooth but biased responses that would leave persistent cumulative drift.

During training, the experimental flow logs were converted into sliding-window samples. The dynamic features, static target-flow input, and PI-gain labels were normalized before training. The datasets were split into training and validation subsets, and one record was reserved for model inference. The resulting channel-specific TV-MTLSTM predictions were $K_p = 0.6128$, $K_i = 0.2463$ for the RP channel and $K_p = 0.9527$, $K_i = 0.3003$ for the UF channel. These predicted gains were then implemented on the physical system and evaluated against the 25 fixed-gain configurations using flow-tracking RMSE, flow-tracking MAE, and maximum absolute cumulative error. Therefore, the term "optimized PI gains" in this thesis refers to the TV-MTLSTM-predicted channel-specific gains that produced the best overall flow-tracking and cumulative-error performance on the tested benchtop platform.

Chapter 4

DESIGN OF THE PORTABLE DIALYSIS PLATFORM

4.1 Design Requirements

The development of the portable dialysis platform for benchtop validation—and its eventual translation toward wearable applications—necessitates a careful balance of engineering, economic, and biomedical constraints. To ensure the prototype effectively supports albumin dialysis research, the following primary design requirements were established:

- **Compact System Size:** Unlike traditional hemodialysis machines that are bulky and largely restricted to clinical settings, this platform requires a reduced footprint. The system must be compact enough to fit conveniently on a standard laboratory benchtop. Furthermore, a small form factor is desirable for improving system integration and supporting future development toward portable and wearable implementations.

- **Low-Cost Implementation:** Commercial dialysis platforms are associated with high operating costs. Therefore, reducing cost was considered an important requirement in the design of the proposed prototype. In the present system, this goal was addressed mainly by using a dialysis strategy with low dialysate volume, which reduces dialysate consumption during each treatment. Lower dialysate use helps decrease the cost of each treatment while maintaining system performance.

- **Stable and Accurate Flow Control:** Precise fluid management is critical for consistent toxin clearance and maintaining transmembrane pressure balance. In this platform, flow regulation is achieved through the precise control of the blood pump and the ultrafiltration pump. To ensure reliable long-term operation, the system's fluidic per-

formance is evaluated against two key metrics: flow rate stability and cumulative total flow error. The platform must actively minimize instantaneous flow fluctuations and prevent volumetric drift over extended durations. Implementing real-time monitoring and closed-loop control is therefore essential to meet these metrics and guarantee high experimental repeatability.

- **Air Intrusion Prevention:** In extracorporeal blood circuits, preventing air intrusion is a paramount safety requirement to mitigate the risk of air embolism. The proposed platform must integrate robust, active bubble management. Specifically, the system must feature an automated fail-safe mechanism: upon the detection of an air bubble, the control unit must immediately halt pump operation and actuate a clamp on the outflow line. This rapid, coordinated response ensures that air-infused blood is strictly prevented from returning to the patient.

- **Modular Architecture and Ease of Operation:** Although the current system was developed as a benchtop prototype, modularity was considered an important design requirement for future clinical and portable applications. The system was designed to allow straightforward assembly, disassembly, and replacement of consumable components such as tubing sets and dialyzers. The use of a cassette architecture simplified setup procedures, including priming, rinsing, and calibration, and improved the practicality of routine operation and maintenance. In addition, the design was intended to support consistent operating conditions across experiments, thereby improving the repeatability and reproducibility of benchtop testing.

4.2 Prototype

The physical prototype of the portable dialysis platform was fabricated using both laser cutting and three-dimensional (3D) printing. This approach was chosen to balance structural rigidity, manufacturing efficiency, and dimensional accuracy.

The main chassis and cassette components were fabricated from clear acrylic sheets by laser cutting, which provided sufficient precision for alignment and assembly. Two acrylic thicknesses were used based on the mechanical requirements of different parts. The main pump mounting plate was made from 5 mm acrylic to provide adequate structural support for the pumps. By contrast, the cassette body and secondary enclosure panels were fabricated from 3 mm acrylic, which provided sufficient stiffness while reducing the overall weight of the device.

Components with more complex three-dimensional geometries were fabricated by fused deposition modeling (FDM) 3D printing. Custom parts, including dialyzer mounting brackets and auxiliary fixtures, were printed using polylactic acid (PLA) filament. PLA was chosen because it provided adequate dimensional consistency and mechanical strength for these components. In addition, 3D printing allowed rapid fabrication of customized parts needed to accommodate the cylindrical dialyzer and the associated tubing.

4.3 System Integration and Control Architecture

The system operated on a standard 110 V AC supply, converted to a primary 24 V DC bus via an external adapter. A DC-DC buck converter then stepped this down to 12 V to power the bubble detector and USB hub.

The powered USB hub provided power and communication connections for several peripheral devices, including an Arduino Nano, two independent scale controllers, and an RS-485 communication module. The RS-485 interface was used to communicate with three dedicated pump controllers, allowing independent control of each pump unit.

To enhance operational safety, the system incorporated a hardware-based shutdown mechanism. The primary 24 V DC bus also supplied a relay module that controlled a solenoid pinch valve. After completion of the priming phase, the bubble detector continuously monitored the fluid line during system operation. If a bubble was detected, the control system immediately initiated a protected shutdown sequence by stopping all active pumps and triggering the relay to actuate the solenoid valve. This action clamped the tubing and

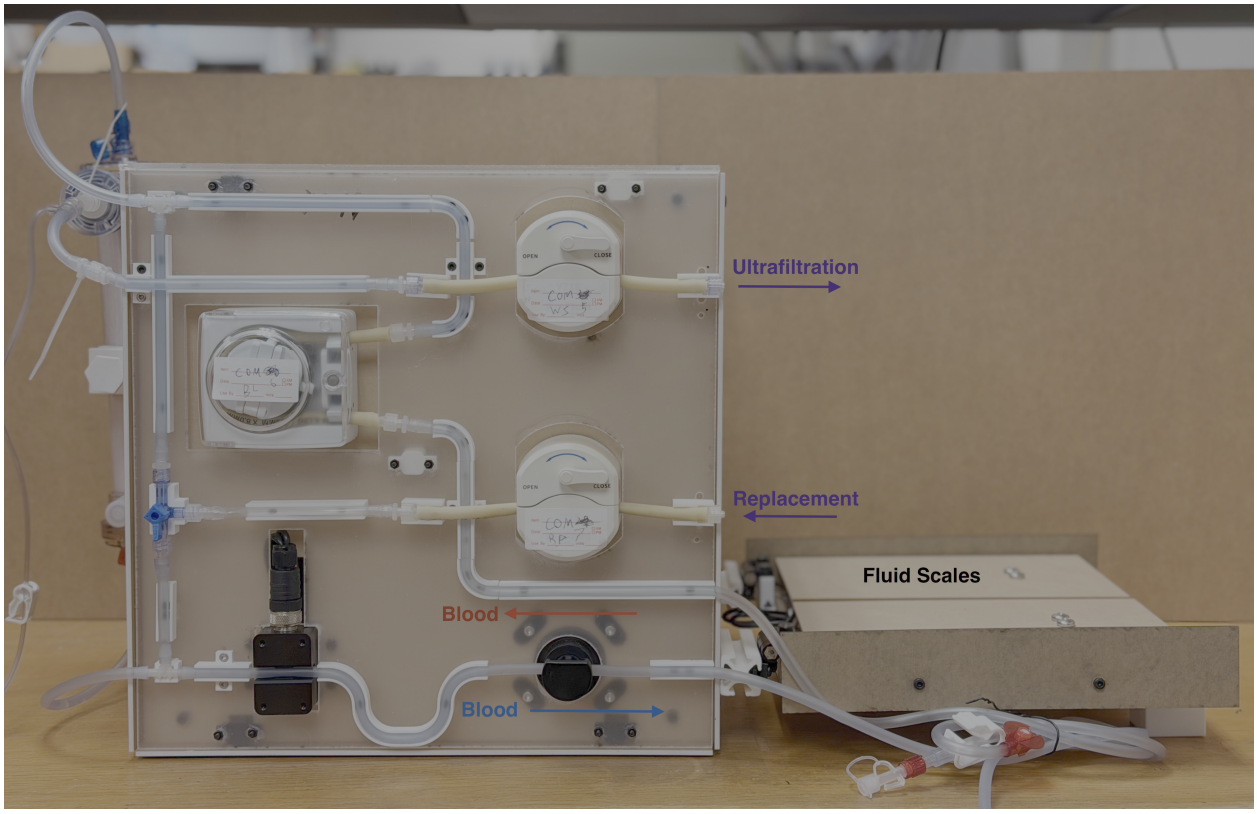

Figure 4.1: Prototype of the portable dialysis platform showing the blood, replacement, and ultrafiltration flow paths, together with the integrated fluid scales.

interrupted fluid transport, thereby placing the system in a safe shutdown state.

4.4 Performance Evaluation and Results

Representative RP and UF flow-control results are shown in Figures 4.2 to 4.5. The selected cases compare the uncontrolled baseline, pure integral control, an intermediate PI setting, and the optimized channel-specific PI gains obtained using the TV-MTLSTM-based procedure described in Section 3.4. The plots provide the corresponding time histories of instantaneous flow and cumulative error, allowing the transient behavior, steady-state deviation, oscillation level, and long-term volumetric accuracy to be evaluated together.

The uncontrolled case ($K_p = 0$, $K_i = 0$) exhibited a systematic offset between the two channels: the RP flow remained above the 40 mL/min target and the UF flow remained below it. This offset produced a nearly monotonic drift in the cumulative error, which indicates that open-loop operation is insufficient for maintaining long-term volumetric balance. When pure integral control was applied ($K_p = 0$, $K_i = 1.0$), the cumulative-error drift was substantially reduced, but the instantaneous flow showed pronounced oscillation, especially in the RP channel. This result indicates that integral action alone can correct the accumulated error but does not provide adequate damping.

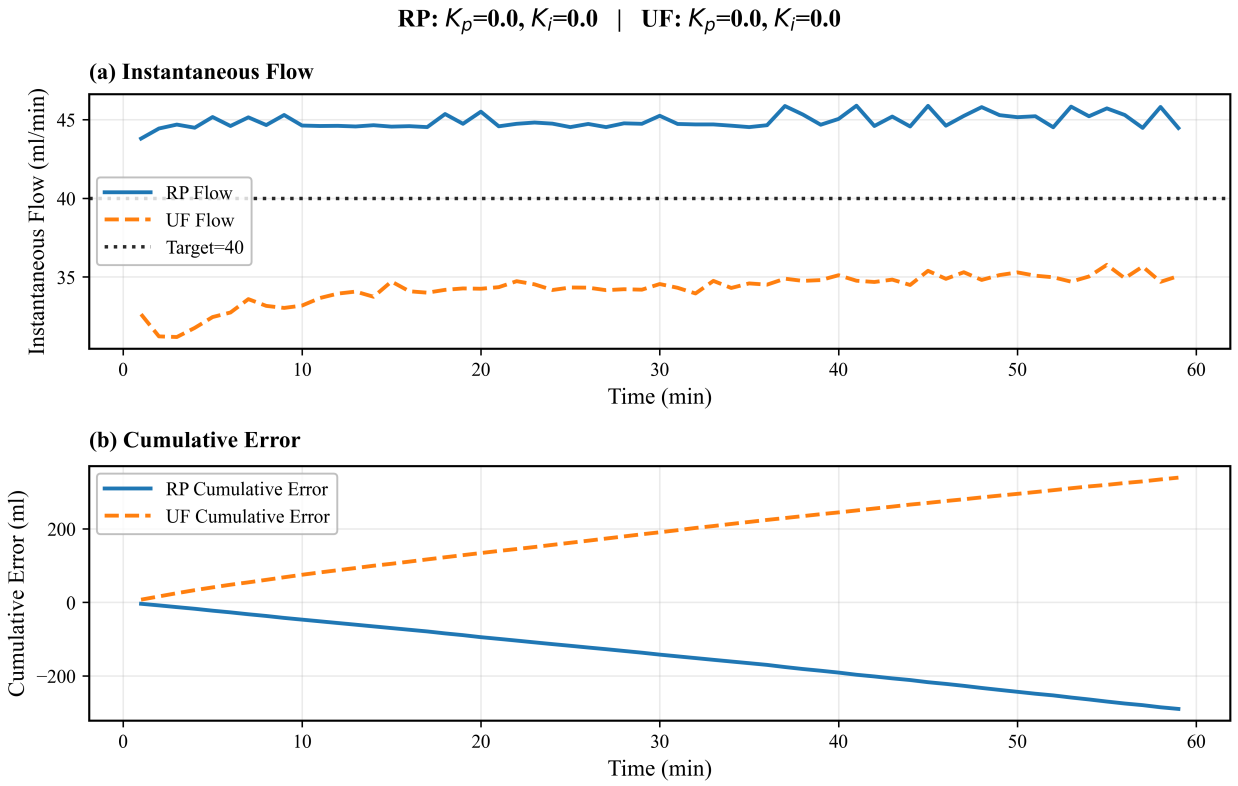

Figure 4.2: Flow-control response without proportional or integral feedback. Both RP and UF channels show persistent offsets from the 40 mL/min target, resulting in nearly monotonic cumulative-error drift over time.

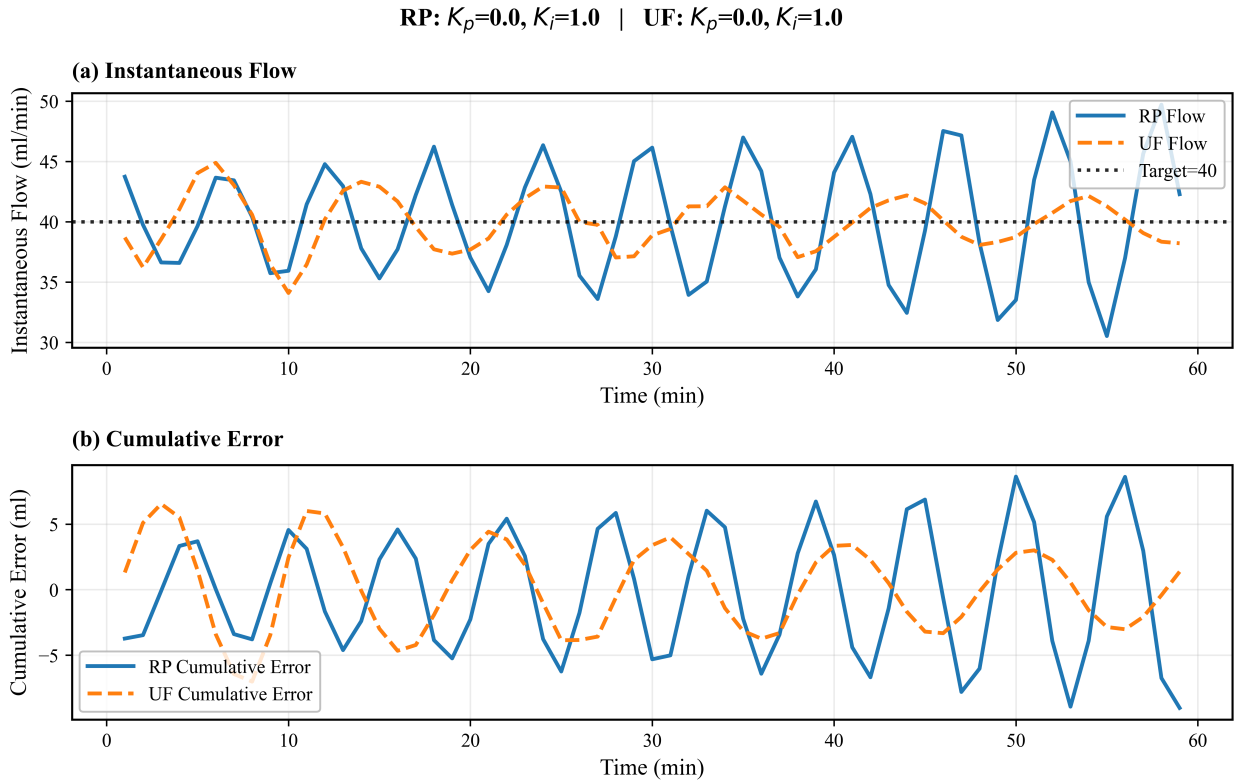

Figure 4.3: Flow-control response under pure integral control with $K_p = 0$ and $K_i = 1.0$. The cumulative-error drift is reduced compared with the uncontrolled case, but the instantaneous flow exhibits pronounced sinusoidal oscillation, especially in the RP channel.

Adding proportional feedback improved the transient response. With $K_p = 0.25$ and $K_i = 0.75$, both channels remained closer to the target and the cumulative errors were bounded near zero, although damped oscillations were still observed. The optimized PI condition, obtained from the TV-MTLSTM gain prediction, provided the most stable response among the selected cases. Using channel-specific gains of $K_p = 0.6128$, $K_i = 0.2463$ for RP and $K_p = 0.9527$, $K_i = 0.3003$ for UF, both channels converged rapidly toward the 40 mL/min target and maintained small cumulative errors without sustained drift or large oscillation.

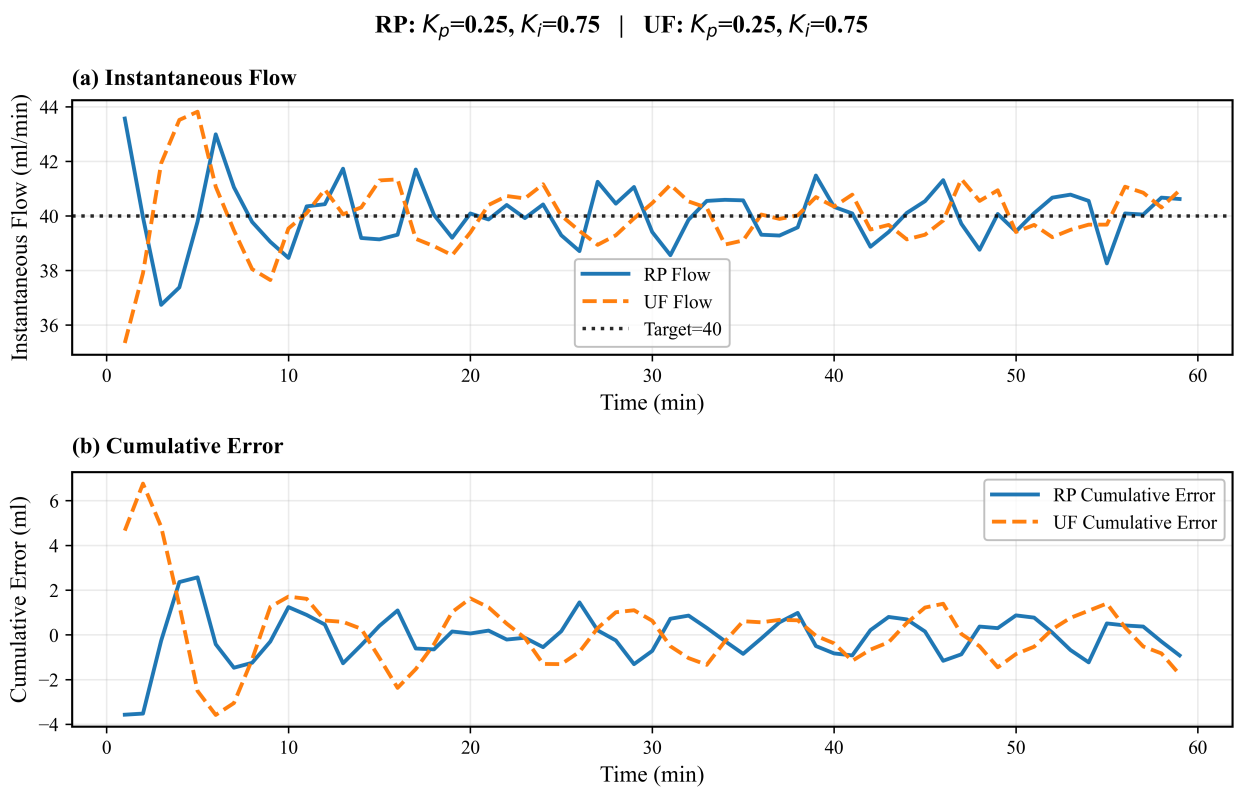

Figure 4.4: Flow-control response with an intermediate PI setting of $K_p = 0.25$ and $K_i = 0.75$. The introduction of proportional feedback reduces the oscillation amplitude and keeps the cumulative errors bounded near zero, although damped oscillatory behavior remains visible.

To quantify this comparison across all 25 fixed-gain configurations and the TV-MTLSTM-predicted condition, three metrics were computed per channel: the instantaneous flow-tracking RMSE and MAE relative to the 40 mL/min target, and the maximum absolute cumulative error. The maximum absolute cumulative error was used rather than only the final cumulative error because it captures the largest cumulative deviation reached during the entire experiment and is therefore less affected by cancellation between positive and negative errors.

As summarized in Table A.1, under the TV-MTLSTM-optimized PI condition, the RP

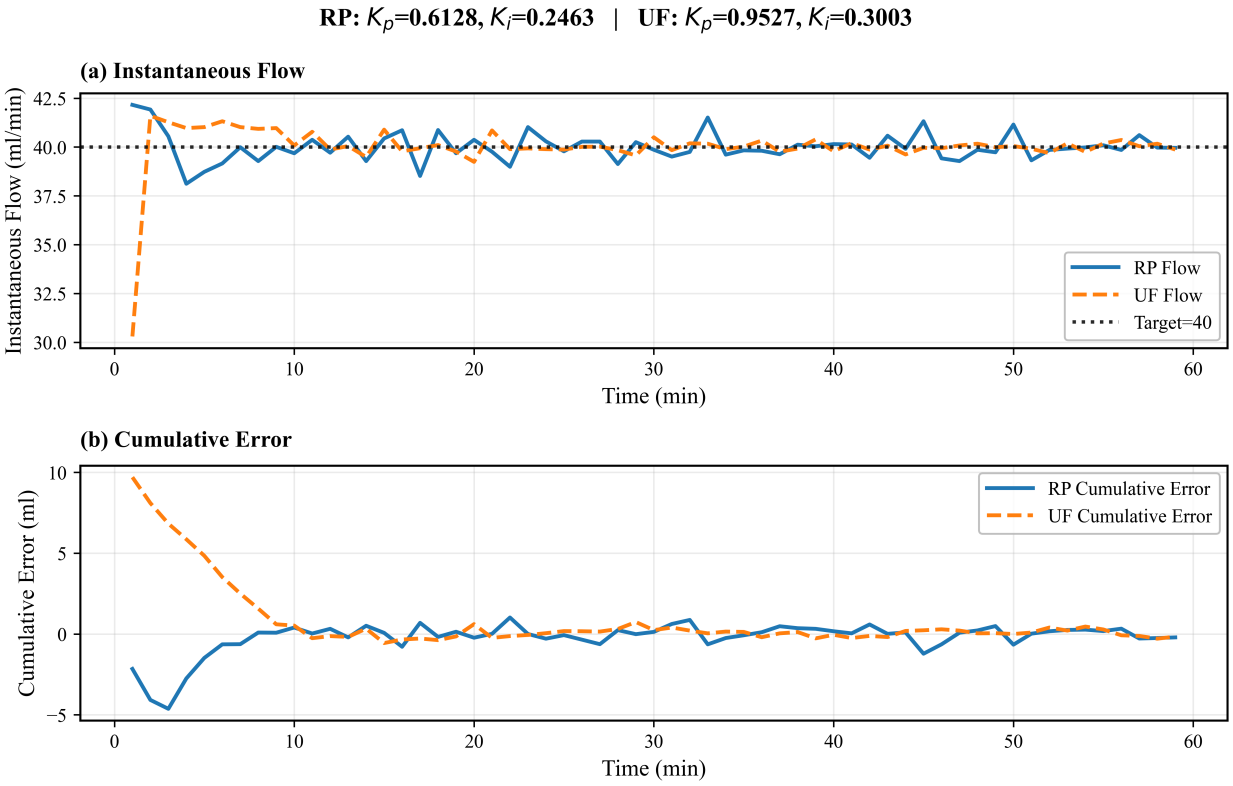

Figure 4.5: Flow-control response under the optimized PI gains. Both RP and UF flows remain close to the 40 mL/min target after the startup transient, and the cumulative errors stay near zero without sustained drift or large oscillation.

channel achieved the lowest instantaneous flow-tracking errors among all RP cases, with an RMSE of 0.737 mL/min and an MAE of 0.535 mL/min. The UF channel similarly achieved the lowest instantaneous errors among UF cases, with an RMSE of 1.363 mL/min and an MAE of 0.505 mL/min. The maximum absolute cumulative error was 4.63 mL for the RP channel, the lowest among all RP cases, and 9.70 mL for the UF channel, the lowest among all UF cases. Taken together, these results indicate that the optimized PI gains minimized instantaneous flow deviation while keeping cumulative error bounded at a low level, supporting the conclusion that the TV-MTLSTM prediction provided the best overall

tradeoff between target-flow tracking, damping, and long-term volumetric balance.

Overall, the selected results reveal a clear progression in controller behavior. Without feedback control, persistent flow offsets produce cumulative-error drift. Pure integral control eliminates most of this drift but introduces significant oscillation. Introducing proportional action improves damping and reduces oscillation, while a properly optimized PI combination yields the most stable and accurate control performance. Therefore, the optimized PI controller was identified as the best-performing configuration because it simultaneously minimized flow deviation from the target, reduced oscillatory behavior, and maintained cumulative error near zero in both channels.

BIBLIOGRAPHY

[1] Raymond Vanholder, Rita De Smet, and Norbert Lameire. Protein-bound uremic solutes: The forgotten toxins. *Kidney International*, 59:S266–S270, February 2001.

[2] Ankit Agarwal and Fatima Anjum. Hemodialysis. In *StatPearls*. StatPearls Publishing, Treasure Island (FL), 2026.

[3] William Bernal and Julia Wendon. Acute Liver Failure. *New England Journal of Medicine*, 369(26):2525–2534, December 2013.

[4] J. Stange, S. Mitzner, W. Ramlow, T. Gliesche, H. Hickstein, and R. Schmidt. A new procedure for the removal of protein bound drugs and toxins. *ASAIO journal*, 39(3):M621–625, 1993.

[5] Radhika Tandon and Saied Froghi. Artificial liver support systems. *Journal of Gastroenterology and Hepatology*, 36(5):1164–1179, 2021.

[6] Alexander Novokhodko, Nanye Du, Shaohang Hao, Ziyuan Wang, Zhiquan Shu, Suhail Ahmad, and Dayong Gao. Predicting the Impact of Polysulfone Dialyzers and Binder Dialysate Flow Rate on Bilirubin Removal. *Bioengineering*, 11(12):1262, December 2024.

[7] T. A. Depner, S. Rizwan, and T. A. Stasi. Pressure effects on roller pump blood flow during hemodialysis. *ASAIO transactions*, 36(3):M456–459, 1990.

[8] Rosemary Ouseph and Richard A. Ward. Increasing Dialysate Flow Rate Increases Dialyzer Urea Mass Transfer-Area Coefficients During Clinical Use. *American Journal of Kidney Diseases*, 37(2):316–320, February 2001.

[9] Suhail Ahmad, Alexander Novokhodko, Iris W. Liou, Nancy Colobong Smith, Robert L. Carithers, Jorge Reyes, Ramasamy Bakthavatsalam, Carl Martin, Renuka Bhattacharya, Nanye Du, Shaohang Hao, and Dayong Gao. Development and First Clinical Use of an Extracorporeal Artificial Multiorgan System in Acute-on-Chronic Liver Failure Patients. *ASAIO journal*, 70(8):690–697, August 2024.

[10] Da-Wei Wang, Yi-Mei Yin, and Yong-Ming Yao. Advances in the management of acute liver failure. *World Journal of Gastroenterology : WJG*, 19(41):7069–7077, November 2013.

[11] Constantine J Karvellas, Noel Gibney, Demetrios Kutsogiannis, Julia Wendon, and Vincent G Bain. Bench-to-bedside review: Current evidence for extracorporeal albumin dialysis systems in liver failure. *Critical Care*, 11(3):215, 2007.

[12] Rajiv Jalan, Kerstin Schnurr, Rajeshwar P. Mookerjee, Sambit Sen, Lisa Cheshire, Stephen Hodges, Vladimir Muravsky, Roger Williams, Gert Matthes, and Nathan A. Davies. Alterations in the functional capacity of albumin in patients with decompensated cirrhosis is associated with increased mortality. *Hepatology*, 50(2):555–564, 2009.

[13] Vicente Arroyo, Rita García-Martinez, and Xavier Salvatella. Human serum albumin, systemic inflammation, and cirrhosis. *Journal of Hepatology*, 61(2):396–407, August 2014.

[14] Jitske Jansen, Joachim Jankowski, Prathibha R. Gajjala, Jack F. M. Wetzels, and Rosalinde Masereeuw. Disposition and clinical implications of protein-bound uremic toxins. *Clinical Science*, 131(14):1631–1647, July 2017.

[15] Raymond Vanholder, Rita De Smet, Griet Glorieux, Angel Argilés, Ulrich Baurmeister, Philippe Brunet, William Clark, Gerald Cohen, Peter Paul De Deyn, Reinhold Deppisch, Beatrice Descamps-Latscha, Thomas Henle, Achim Jörres, Horst Dieter Lemke, Ziad A. Massy, Jutta Passlick-Deetjen, Mariano Rodriguez, Bernd Stegmayr, Peter Stenvinkel, Ciro Tetta, Christoph Wanner, Walter Zidek, and European Uremic Toxin Work Group (EUTox). Review on uremic toxins: Classification, concentration, and interindividual variability. *Kidney International*, 63(5):1934–1943, May 2003.

[16] Jan Stange. Extracorporeal liver support. *Organogenesis*, 7(1):64–73, 2011.

[17] Antonio Santoro. Confounding factors in the assessment of delivered hemodialysis dose. *Kidney International*, 58:S19–S27, August 2000.

[18] Evangelos Tsipotis, Asim Shuja, and Bertrand L. Jaber. Albumin Dialysis for Liver Failure: A Systematic Review. *Advances in Chronic Kidney Disease*, 22(5):382–390, September 2015.

[19] Yuanyuan Shi, Huajun Tian, Yifeng Wang, Yue Shen, Qiuyu Zhu, and Feng Ding. Improved Dialysis Removal of Protein-Bound Uraemic Toxins with a Combined Displacement and Adsorption Technique. *Blood Purification*, 51(6):548–558, June 2022.

[20] Zaccaria Ricci, Stefano Romagnoli, Thiago Reis, Rinaldo Bellomo, and Claudio Ronco. Hemoperfusion in the intensive care unit. *Intensive Care Medicine*, 48(10):1397–1408, 2022.

[21] Claudio Ronco and Rinaldo Bellomo. Hemoperfusion: Technical aspects and state of the art. *Critical Care*, 26:135, May 2022.

[22] Philippe R. Bauer, Marlies Ostermann, Lene Russell, Chiara Robba, Sascha David, Bruno L. Ferreyro, Joan Cid, Pedro Castro, Nicole P. Juffermans, Luca Montini, Tasneem Pirani, Andry Van De Louw, Nathan Nielsen, Julia Wendon, Anne C. Brignier, Miet Schetz, Jan T. Kielstein, Jeffrey L. Winters, and Elie Azoulay. Plasma exchange in the intensive care unit: A narrative review. *Intensive Care Medicine*, 48(10):1382–1396, 2022.

[23] Juan José García Martínez and Karim Bendjelid. Artificial liver support systems: What is new over the last decade? *Annals of Intensive Care*, 8:109, November 2018.

[24] Frank J.-G. Luo, Kajal P. Patel, Ilian O. Marquez, Natalie S. Plummer, Thomas H. Hostetter, and Timothy W. Meyer. Effect of Increasing Dialyzer Mass Transfer Area Coefficient and Dialysate Flow on Clearance of Protein-Bound Solutes: A Pilot Crossover Trial. *American Journal of Kidney Diseases*, 53(6):1042–1049, June 2009.

[25] Maaike K van Gelder, Alferso C Abrahams, Jaap A Joles, George A Kaysen, and Karin G F Gerritsen. Albumin handling in different hemodialysis modalities. *Nephrology Dialysis Transplantation*, 33(6):906–913, June 2018.

[26] Martin Boyle, Jelica Kurtovic, David Bihari, Stephen Riordan, and Christian Steiner. Equipment review: The molecular adsorbents recirculating system (MARS®). *Critical Care*, 8(4):280–286, 2004.

[27] R. D. Hughes. Review of methods to remove protein-bound substances in liver failure. *The International Journal of Artificial Organs*, 25(10):911–917, October 2002.

[28] Christoph Sponholz, Katja Matthes, Dina Rupp, Wolf Backaus, Sebastian Klammt, Diana Karailieva, Astrid Bauschke, Utz Settmacher, Matthias Kohl, Mark G. Clemens, Steffen Mitzner, Michael Bauer, and Andreas Kortgen. Molecular adsorbent recirculating system and single-pass albumin dialysis in liver failure – a prospective, randomised crossover study. *Critical Care*, 20(1):2, January 2016.

[29] Wisit Cheungpasitporn, Charat Thongprayoon, Ziad M. Zoghby, and Kianoush Kashani. MARS: Should I Use It? *Advances in Chronic Kidney Disease*, 28(1):47–58, January 2021.

[30] Alexander Novokhodko, Shaohang Hao, Suhail Ahmad, and Dayong Gao. Non-Cell-Based Extracorporeal Artificial Liver Systems: Historic Perspectives, Approaches and Mechanisms, Current Applications, and Challenges. *Artificial Organs*, 49(6):925–944, June 2025.

[31] Richard A. Ward and Claudio Ronco. Dialyzer and machine technologies: Application of recent advances to clinical practice. *Blood Purification*, 24(1):6–10, 2006.

[32] John K. Leypoldt, Craig D. Kamerath, Janice F. Gilson, and Goetz Friederichs. Dialyzer clearances and mass transfer-area coefficients for small solutes at low dialysate flow rates. *ASAIO journal*, 52(4):404–409, 2006.

[33] Shintaro Hamada, Masami Hata, Shuntaro Furukawa, and Sunao Yamamoto. Effectiveness of blood volume change-guided ultrafiltration control (BV-UFC) in hemodialysis: A crossover comparative study. *Clinical Kidney Journal*, 18(5):sfaf141, May 2025.

[34] Hans-Dietrich Polaschegg. Hemodialysis machine technology: A global overview. *Expert Review of Medical Devices*, 7(6):793–810, November 2010.

[35] Hitesh K. Mehta, Diane Deabreu, James G. McDougall, and Marc B. Goldstein. Correction of discrepancy between prescribed and actual blood flow rates in chronic hemodialysis patients with use of larger gauge needles. *American Journal of Kidney Diseases*, 39(6):1231–1235, June 2002.

[36] M. Roberts and R. J. Winney. Errors in fluid balance with pump control of continuous hemodialysis. *The International Journal of Artificial Organs*, 15(2):99–102, February 1992.

[37] Antonio Santoro, Elena Mancini, Carlo Basile, Luigi Amoroso, Salvatore Di Giulio, Mario Usberti, Giuliano Colasanti, Giuseppe Verzetti, Alessandro Rocco, Enrico Imbasciati, Giovanni Panzetta, Roberto Bolzani, Fabio Grandi, and Maurizio Polacchini. Blood volume controlled hemodialysis in hypotension-prone patients: A randomized, multicenter controlled trial. *Kidney International*, 62(3):1034–1045, September 2002.

[38] Fokko P. Wieringa, Swathi Suran, Henning Søndergaard, Stephen Ash, Cian Cummins, Ashesh Ray Chaudhuri, Tugrul Irmak, Karin Gerritsen, and Jeroen Vollenbroek. The Future of Technology-Based Kidney Replacement Therapies: An Update on Portable, Wearable, and Implantable Artificial Kidneys. *American Journal of Kidney Diseases*, 85(6):787–796, June 2025.

[39] John Daugirdas, Peter Blake, and Todd Ing. Handbook of Dialysis (5th ed.). *Faculty Bookshelf*, January 2015.

[40] Joseph V. Bonventre, Frank P. Hurst, Melissa West, Iwen Wu, Prabir Roy-Chaudhury, and Murray Sheldon. A Technology Roadmap for Innovative Approaches to Kidney Replacement Therapies: A Catalyst for Change. *Clinical journal of the American Society of Nephrology: CJASN*, 14(10):1539–1547, October 2019.

[41] David Loureiro Ramada, Joost de Vries, Jeroen Vollenbroek, Nazia Noor, Odyl Ter Beek, Silvia M. Mihăilă, Fokko Wieringa, Rosalinde Masereeuw, Karin Gerritsen, and Dimitrios Stamatialis. Portable, wearable and implantable artificial kidney systems: Needs, opportunities and challenges. *Nature Reviews. Nephrology*, 19(8):481–490, August 2023.

[42] Alan S. Kliger. Maintaining Safety in the Dialysis Facility. *Clinical Journal of the American Society of Nephrology : CJASN*, 10(4):688–695, April 2015.

[43] Keiko I. Greenberg and Michael J. Choi. Hemodialysis Emergencies: Core Curriculum 2021. *American Journal of Kidney Diseases*, 77(5):796–809, May 2021.

[44] Oksana Harasemiw, Clara Day, John E. Milad, James Grainger, Thomas Ferguson, and Paul Komenda. Human factors testing of the Quanta SC+ hemodialysis system: An innovative system for home and clinic use. *Hemodialysis International*, 23(3):306–313, 2019.

[45] Flore Duranton, Gerald Cohen, Rita De Smet, Mariano Rodriguez, Joachim Jankowski, Raymond Vanholder, and Àngel Argilés. Normal and pathologic concentrations of uremic toxins. *Journal of the American Society of Nephrology*, 23(7):1258–1270, 2012.

Appendix A

SUPPLEMENTARY FIGURES AND TABLES

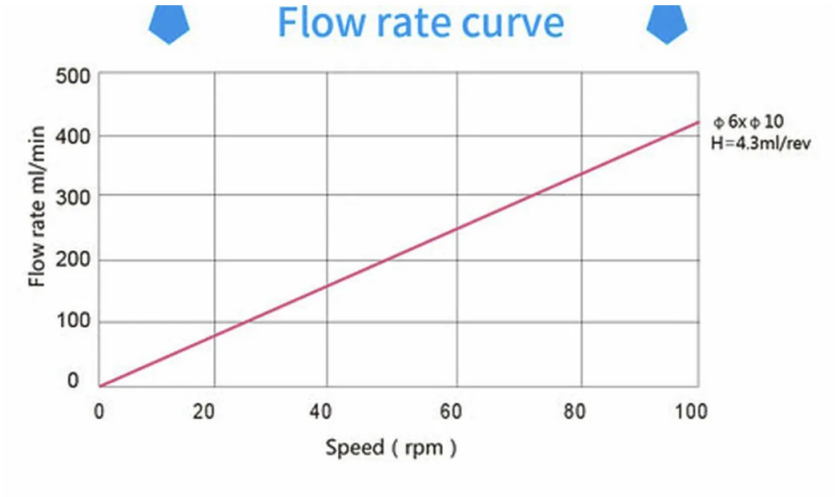

OEM DC brushless motor-TH152 Flow Curve

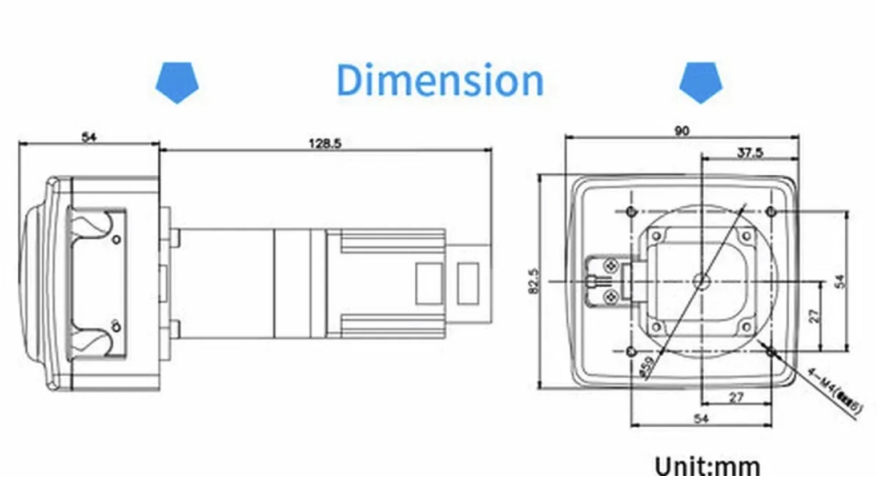

OEM DC brushless motor-TH152 Dimension

Figure A.1: Flow rate–speed characteristics and dimensional specifications of the OEM DC brushless motor (TH152) used in the system.

Table A.1: Summary metrics for all tested PI combinations in the RP and UF channels. The bold rows indicate the TV-MTLSTM-predicted PI settings for the corresponding channel.

K_p	K_i	RP channel			UF channel		
		RMSE (mL/min)	MAE (mL/min)	Max. cum. err. (mL)	RMSE (mL/min)	MAE (mL/min)	Max. cum. err. (mL)
0	0	4.933	4.911	289.77	5.829	5.749	339.20
0	0.25	6.406	5.741	21.85	3.202	2.143	40.30
0	0.5	5.175	4.629	12.53	3.706	3.127	24.50
0	0.75	6.834	6.166	13.52	2.898	2.160	21.25
0	1	8.868	7.893	16.23	2.873	2.166	18.27
0.25	0	1.516	0.783	37.79	3.415	1.949	110.74
0.25	0.25	2.003	1.069	14.61	2.709	1.632	35.27
0.25	0.5	1.987	1.110	11.58	2.431	1.409	23.38
0.25	0.75	2.041	1.225	9.96	2.474	1.681	19.15
0.25	1	2.697	1.669	9.81	2.306	1.317	18.29
0.5	0	1.211	0.613	20.02	2.417	1.165	56.87
0.5	0.25	1.566	0.818	12.10	2.328	1.254	25.67
0.5	0.5	1.559	0.795	10.07	2.239	1.067	20.39
0.5	0.75	1.347	0.770	6.96	2.472	1.489	20.87
0.5	1	1.795	0.994	9.19	2.068	1.017	15.71
0.75	0	1.403	0.630	15.91	2.530	1.051	50.55
0.75	0.25	1.418	0.736	11.25	2.250	1.088	23.93
0.75	0.5	1.439	0.700	8.75	2.055	0.925	17.42
0.75	0.75	1.505	0.727	8.47	2.035	0.996	15.65
0.75	1	1.197	0.713	6.35	1.988	1.000	12.37
1	0	1.251	0.574	11.81	2.139	0.815	36.12
1	0.25	1.241	0.564	8.48	1.844	0.814	17.15
1	0.5	1.269	0.640	7.99	2.023	0.855	16.99
1	0.75	1.493	0.778	8.65	1.972	0.893	14.08
1	1	1.279	0.761	6.73	1.903	0.898	11.88
0.6128	**0.2463**	**0.737**	**0.535**	**4.63**	–	–	–
0.9527	**0.3003**	–	–	–	**1.363**	**0.505**	**9.70**

VITA

Jianya Wei received his Bachelor of Engineering degree from Anhui University. He pursued his Master of Science degree in Mechanical Engineering at the University of Washington under the supervision of Professor Dayong Gao.

His master's research focused on the development and evaluation of a portable and fully automated artificial kidney system, with emphasis on albumin dialysis, flow control, pump calibration, and prototype integration. His research interests include mechanical engineering, biomedical engineering, artificial organs, and automated medical devices.